Effect of Spermine Conjugation on the Cytotoxicity and Cellular Transport of Acridine

Jean-Guy Delcros,*[,†] Sophie Tomasi,[‡] Simon Carrington,[§] Bénédicte Martin,[†] Jacques Renault,[‡] Ian S. Blagbrough,[§] and Philippe Uriac[‡]

Groupe de Recherche en Thérapeutiques Anticancéreuses, UPR ESA CNRS 6027, Faculté de Médecine, UPRES EA 2234, Faculté de Pharmacie, Université Rennes 1, 2 Avenue du Professeur Léon Bernard, 35043 Rennes Cédex, France, and Department of Pharmacy and Pharmacology, University of Bath, Bath BA2 7AY, United Kingdom

Polyamines are believed to be potent vectors for the selective delivery of chemotherapeutic agents into cancer cells. In this paper, we report the effect of spermine conjugation on the cytotoxic and transport properties of acridine. Six derivatives, composed of a spermine chain attached at its N^1 position to an acridine via an aliphatic chain, were synthesized. The aliphatic linker, comprised of 3–5 methylene units, was connected to the position-9 of the heterocycle through either an amide (amidoacridines **8**–**10**) or an amine (aminoacridines **11**–**13**) linkage. Independently of their architecture, all ligands showed a high affinity for DNA binding but a limited DNA sequence selectivity. In a whole cell assay with L1210 and Chinese hamster ovary (CHO) cells, the aminoacridines (IC_{50} values around 2 μM) were more potent than the amidoacridines (IC_{50} values between 20 and 40 μM). This was related to a less efficient transport for the latter. As determined from competitive uptake studies with [^{14}C]spermidine, all conjugates had a high affinity for the polyamine transport system (PTS). However, on the basis of competitive studies with an excess of spermidine and on the differential effect on cell growth and accumulation in CHO and in the mutant PTS deficient CHO-MG cells, the accumulation of the conjugates through the PTS was found to be poor but still more efficient for the aminoacridines. α-Difluoromethylornithine (DFMO), an inhibitor of ornithine decarboxylase, which induces an up-regulation of the activity of the PTS, enhanced accumulation of all acridine conjugates through the PTS and had a synergistic effect on the potency of the acridine conjugates to inhibit cell growth. Despite their high affinity for the PTS, the low amount of derivatives transiting through the PTS is likely to be related to their ability to repress rapidly and efficiently the activity of the PTS and, consequently, to inhibit their own uptake via this system.

Introduction

Natural polyamines, such as spermine (**1**) and spermidine (**2**) are ubiquitous polycationic molecules, which play crucial roles in a number of cell processes including cell proliferation and differentiation.[1] In eukaryotic cells, intracellular polyamine pool size is determined by highly regulated complex biosynthetic and catabolic pathways as well as by specific active transport systems allowing polyamine exchange (uptake and release) with the environment. Intracellular levels of free polyamines control the activity of the uptake system as well as the anabolic pathways.[2–4] Structural features of polyamines, the high need of tumor cells for these polycations, along with the characteristics of their cell transport systems make polyamines attractive vectors for tumor targeting.[4] The activity of the polyamine transport system (PTS) is higher in highly proliferating cells such as tumor cells than in resting cells.[5,6] Depletion of intracellular polyamine pools, e.g., by α-difluoromethylornithine (DFMO), a suicide substrate inhibitor of ornithine decarboxylase, greatly enhances polyamine uptake by various cell lines.[7–9] In vivo, tissues with a

high demand for polyamines such as tumors take up radiolabeled polyamines in greater amounts than other tissues.[10,11] As the polyamine content of tumor cells is more efficiently depleted by DFMO than that of non- or slow-growing cells, DFMO increases the uptake rate of tumor cells that readily accumulate high amounts of polyamines.[10–13]

The selectivity of the PTS is not restricted to natural polyamines. Indeed, polyamine uptake systems have a low stringency for structural features thereby allowing a wide variety of synthetic polyamine analogues to be taken up by these systems.[4] The PTS may therefore afford an alternative mode of entry into cells for more selective chemotherapeutics. The vectorization of chemotherapeutic drugs by polyamines is expected to enhance cytotoxicity to tumor cells and diminish secondary effects on normal cells. These characteristics have led to the design of polyamine conjugated to known chemotherapeutic drugs. For example, chlorambucil,[14–16] nitroimidazole,[17] and aziridine[18–20] polyamine conjugates have been synthesized with improved therapeutic indexes. However, evidence concerning the ability of these conjugates to use the PTS is mostly based on indirect arguments: (i) their ability to inhibit the transport of radiolabeled polyamines, (ii) the synergistic effect of DFMO, or (iii) reduced cytotoxicity in the presence of exogenous polyamines. However, impermeant

---

* To whom correspondence should be addressed. Tel: 33(0)2.23.23.45.03. Fax: 33(0)2.23.23.46.08. E-mail: delcros@univ-rennes1.fr.
† Faculté de Médecine, Université Rennes 1.
‡ Faculté de Pharmacie, Université Rennes 1.
§ University of Bath.

polyamine analogues with high affinity for the polyamine transport have been reported.[21] On the other hand, bis(benzyl)polyamine analogues inhibit polyamine uptake but are substrates for a cell transport system distinct from the PTS.[22,23] In addition, the cytotoxicity of therapeutic drugs unrelated to polyamines, such as BCNU, is enhanced by DFMO.[24] Recent studies with fluorescein−polyamine conjugates have however suggested a broad structural tolerance, the initial velocity of transport of these conjugates being similar to that of the free polyamine homologues.[25]

Among many targets, DNA has been considered as a choice target for anticancer strategy. Disrupting DNA functions or structure will block cell proliferation or kill cells. Numerous DNA intercalating or groove binding agents are potent cytotoxic drugs.[26] Because of the lack of specificity of the target, the activity of DNA targeting drugs may be improved by increasing their selectivity for tumor cells as well as their affinity for DNA. Tethering DNA targeting drugs to polyamines may respond to both imperatives. SPM and SPD have a high affinity for DNA, and despite a limited DNA sequence selectivity,[27] they may be involved in vivo in DNA conformational changes and chromatin condensation.[28] Coupling a polyamine to a DNA targeting agent is believed to increase its DNA binding affinity through electrostatic interactions. The conjugation of the aromatic nitrogen mustard chlorambucil, a clinically important chemotherapeutic agent, to SPD enhances by a factor close to 10^4 its efficiency of cross-linking without altering its preferred cross-linking site.[14,29] The presence of a polyamine side chain on intercalating agents such as anthracene or acridine (**3** and **4**) does not prevent the intercalating capability of the drug although the geometry of the complex is slightly altered, and also, it does allow the conjugate to have higher affinity by using additional nonintercalative binding modes.[30−32] It has also been shown that polyamine conjugation does not disrupt the topoisomerase II inhibitory activity of acridine.[33,34] Taken together, these data suggest that tethering a polyamine chain to a DNA binding agent will not alter and possibly may improve its activity.

Recently, Phanstiel and collaborators[33,34] raised the question as to whether polyamine conjugation to bulky DNA binding agents such as linear tricyclic systems (**5** and **6**) may improve their selectivity by targeting the PTS. On the basis of a SPD protection assay, it was concluded that the monoalkylated SPM motif present in **6** was a better vector than its SPD homologue **5**. This same issue is further addressed in the present work. Our novel analogues are composed of a SPM covalently bound to an acridine via an aminoaliphatic linker. The linker was attached to the 9-position of acridine, through either an amide bond (amidoacridines **8**−**10**) or directly as the aniline (aminoacridines **11**−**13**). The architecture of the conjugates was based on the following observations: (i) Because N^1 derivatives of polyamines show a higher affinity for the polyamine transporter than their N^4 homologues,[35−38] the SPM moiety was linked through one of its terminal amino groups. (ii) Earlier studies demonstrated a relationship between the number of protonated nitrogens along polyamines and their derivatives, and their affinity for the PTS[35,39,40] as well as for DNA.[27] To preserve the full cationic charge of
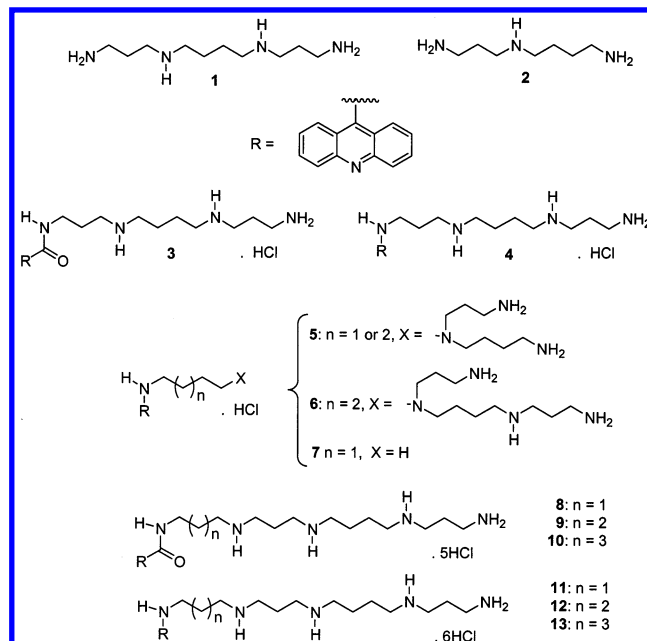

Figure 1. Structures of spermine (**1**), spermidine (**2**), Blagbrough's conjugates (**3** and **4**), Phanstiel's conjugates (**5**−**7**), and our acridine−spermine conjugates (**8**−**13**).

SPM, the linker was bound to SPM via an amine bond. In the present work, conjugates **8**−**13** were studied for their DNA binding properties, cell growth inhibitory effects, and their interactions with the PTS.

Chemical Syntheses

The SPM−acridine conjugates **8**−**13** (Figure 1) differ in two main characteristics: the bond (amide or amine) and the length of the spacer (3−5 methylenes) between the acridine and the SPM moieties. They were obtained by conjugation of three unsymmetrically protected SPM derivatives to acridine-9-carboxylic acid or 9-phenoxyacridine.

As shown in Scheme 1, the synthesis began by the Swern oxidation[41−43] of the N-CBZ-3-aminopropan-1-ol **14** affording the desired aldehyde **17** in 50% yield. The oxidation of N-CBZ-4-aminobutan-1-ol **15** and of N-CBZ-5-aminopentan-1-ol **16** led to the unexpected N-CBZ-cyclic aminals **18** and **19** in 87 and 73%, respectively. The cyclic structures were assessed by ^{13}C NMR spectroscopic data: we observed two signals at 81.2 and 82.0 ppm (mixture of conformational isomers) for compound **18**. These chemical shifts could not be assigned to an aldehydic carbon (201.22 ppm for **17**). They are described as equivalent to the corresponding aminoaldehyde because of their existence in equilibrium with the required aldehyde.[44−48] To our knowledge, this is the first report of the generation of these aminals by oxidation of the corresponding amino alcohols. The existence of this equilibrium was proved by the successful reductive alkylation of **18** and **19** with the N^1,N^4,N^9-tri-*tert*-butoxycarbonylspermine (H₂NA = **20**).[49] They reacted in MeOH in the presence of NaBH₃CN. The pH of the reaction was maintained between 6.0 and 7.5 by the dropwise addition of glacial AcOH. The unsymmetrical polyamine moieties **22** and **23** were obtained after 48 or 72 h in 40 and 29%, respectively. The reductive amination of **20** with the aminoaldehyde
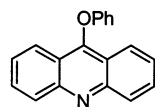
Scheme 1[a]
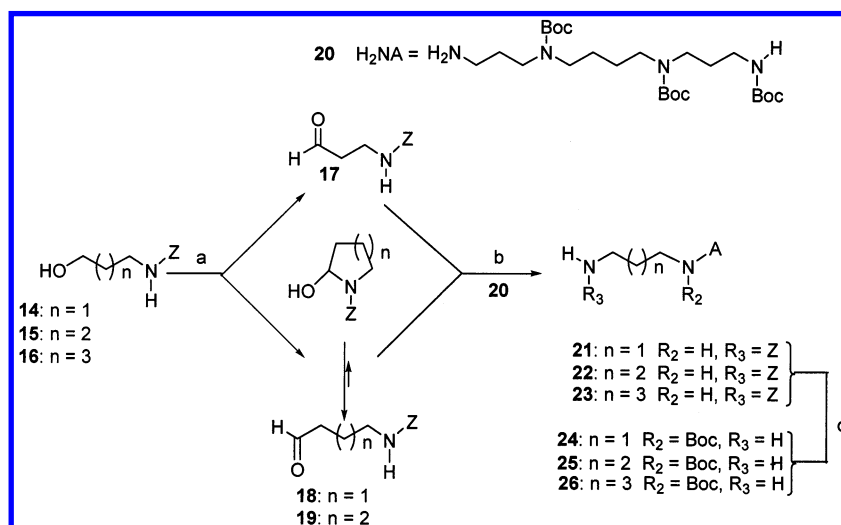
[a] Reagents: (a) DMSO, (COCl)$_2$, Et$_3$N, anhydrous CH$_2$Cl$_2$, −78 °C. (b) NaBH$_3$CN, glacial acetic acid, 4 Å molecular sieves, anhydrous MeOH. (c) (Boc)$_2$O, DMF and then H$_2$, 1 atm, Pearlman's catalyst, MeOH.

Scheme 2[a]
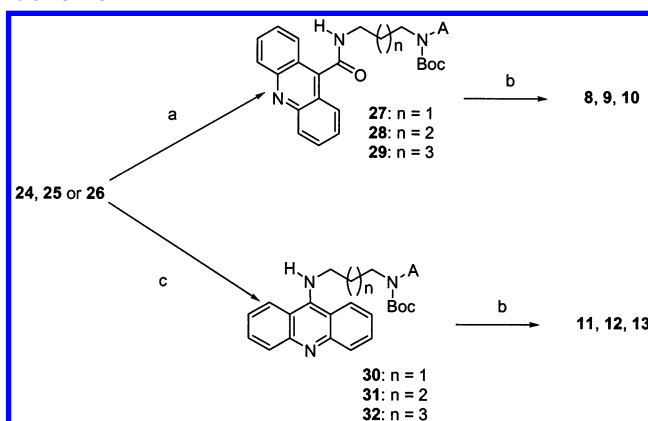
[a] Reagents: (a)
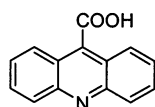
DCC, HOBt, DMF. (b) 0.9 M HCl/EtOAc. (c)

PhOH, Δ.

17 was faster (24 h) and gave the required polyamine **21** in a higher yield (54%).

The last step before the condensation with acridine derivatives was the BOC protection of the free amino group followed by the removal of the CBZ group by Pearlman's catalyst under H$_2$. We obtained the desired BOC-protected polyamines **24**−**26** in 63, 32, and 34%, respectively.

As shown in Scheme 2, the coupling between protected polyamine and acridine moieties involved two different routes. The acylation of **24**−**26** with acridine-9-carboxylic acid was mediated by DCC and a catalytic amount of N^1-hydroxybenzotriazole affording the compounds **27**−**29** in 64, 54, and 67%, respectively. The compounds **30**−**32** were obtained in 65, 54, and 59%,

respectively, by alkylation of the polyamines **24**−**26** with the previously prepared 9-phenoxyacridine.[50−52] The target hydrochlorides **8**−**13** were then generated in good yields using a 0.9 M solution of HCl gas in ethyl acetate.

Biological Studies

1. Optical Properties. All six acridine conjugates absorbed light between 350 and 450 nm and emitted fluorescence. The characteristics of their absorption and fluorescence spectra were (i) dependent on the nature of the bond (amine or amide) between the linker and the acridine heterocycle, (ii) insensitive to the length of the tether, and (iii) modified upon binding to DNA. As an illustration, absorption and fluorescence excitation and emission spectra of conjugates **10** and **11** in the absence and presence of calf thymus DNA (CT-DNA) are shown in Figure 2. Free amidoacridines showed a maximal absorption at 359 nm while two absorption bands (λ_{max} = 410 and 430 nm) were observed for the aminoacridines. Fluorescence spectra of the amido-acridines at pH 7 showed an excitation spectrum centered at 359 nm and a maximum emission at 435 nm. In acidic medium (0.2 N HClO$_4$), the excitation spectra showed two bands (λ_{max} = 360 and 410 nm) and the emission maximum was shifted to 492 nm. For the aminoacridines, emission maxima at 449 and 466 nm were seen at pH 7 as well as in the acidic medium (data not shown). In the presence of CT-DNA, spectral changes were observed as reported for other acridine derivatives.[53,54] This involved a hypochromic effect and bathochromic shifts (λ_{max} = 362 nm for the amido-acridines; λ_{max} = 415 and 440 nm for the aminoacridines) with clear isosbestic points observed at 400 and 445 nm for the aminoacridines and amidoacridines, respectively. Bathochromic shifts clearly sign the binding of individual ligands to the DNA substrate, and isosbestic points are indicative of equilibrium between bound and free molecules. Hypochromism and decrease in the fluorescence emission intensity in the presence of CT-DNA indicate that the DNA-bound acridine derivatives are in a less polar environment.[30,31,55,56]
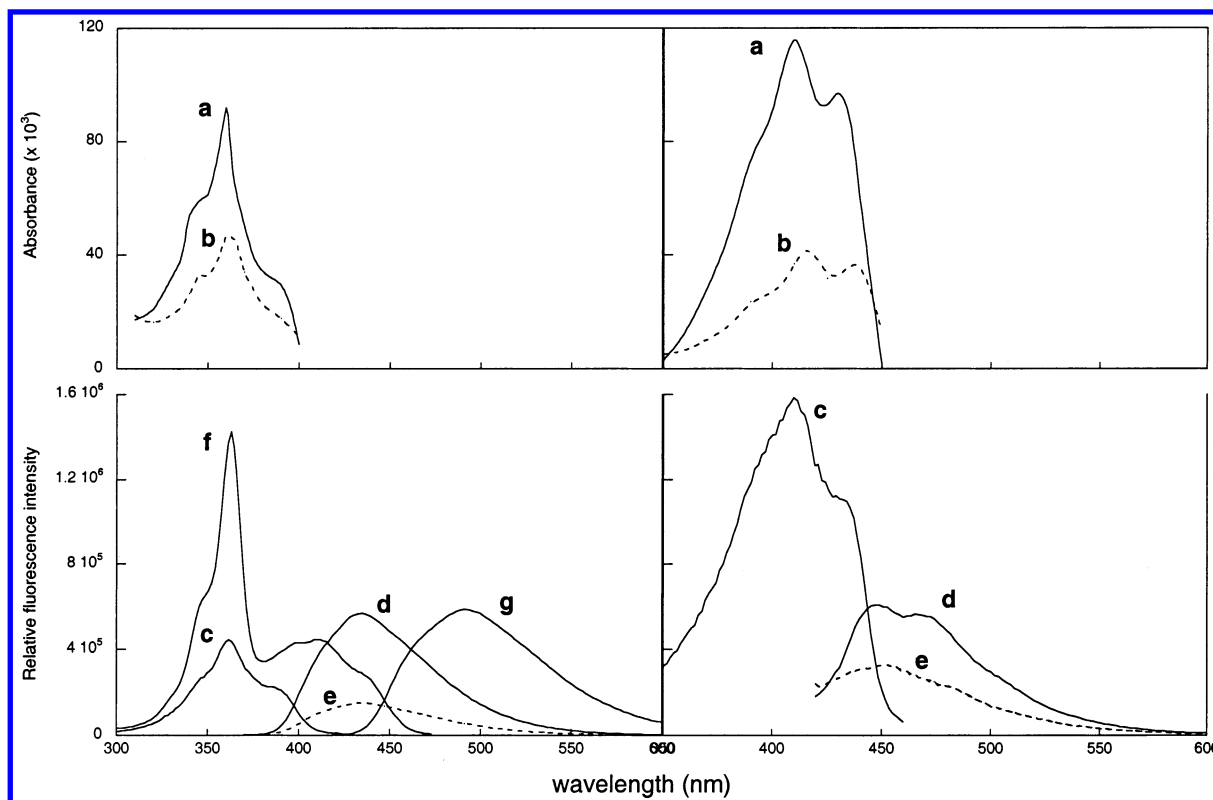
Figure 2. Absorption (upper panels) and fluorescence excitation and emission spectra (lower panels) of the conjugates **10** (left panels) and **11** (right panels). Upper panels: Visible absorption spectra of 10 μM solution of the conjugates in 10 mM Tris-HCl (pH 7.4), 50 mM NaCl in the absence (a) or in the presence of 100 μM CT-DNA (b). Lower panels: Fluorescence excitation (c and f) and emission (d, e, and g) spectra of 0.25 μM solutions of the conjugates either in 10 mM Tris-HCl (pH 7.4), 50 mM NaCl in the absence (c and d) or in the presence of 30 μM CT-DNA (e) or in 0.2 N HClO$_4$ (f and g).

Table 1. DNA Binding Data[a]

compd	Q (μM)[b]			CC$_{50}$ (μM)[c]
	AT	CT-DNA	GC	
8	1.7	1.8	2.0	0.12
9	1.8	1.9	2.1	0.12
10	1.9	2.0	2.1	0.12
11	1.8	2.0	2.2	0.11
12	1.9	2.0	2.4	0.11
13	1.7	1.8	2.3	0.11
SPM **1**	nd[e]	nd	nd	6.8
acridine[d]	26	24	22	142

[a] AT, CT-DNA, and GC refer to [poly(dA-dT)]$_2$, calf thymus DNA, and [poly(dG-dC)]$_2$, respectively. [b] Conjugate concentration to give 50% fluorescence quenching of bound ethidium at pH 5 for an [ethidium]:[DNA] ratio of 0.1:1; mean value ($\pm$10%) from three determinations. [c] Drug concentration to give 50% drop in fluorescence of bound ethidium for an [ethidium]:[CT-DNA] ratio of 1.26:1; mean value ($\pm$5%) from three determinations. [d] Data taken from ref 58. [e] nd, not determined.

2. DNA Binding Properties. "Apparent" equilibrium constants (K_{app}) of drug binding to DNA can be estimated by measuring the loss of ethidium fluorescence consecutive to the displacement of the DNA-bound fluorochrome (at a high [ethidium]:[DNA] molar ratio, e.g., 1.26:1) as a function of added drug. The drug concentration producing 50% inhibition of fluorescence (CC$_{50}$) is approximately inversely proportional to the binding constant.[57] From Table 1, the CC$_{50}$ values determined for ethidium displacement from CT-DNA were found to be around 0.11 μM for all six acridine conjugates and 6.8 μM for free spermine. For untethered acridine, a CC$_{50}$ value of 142 μM has been previously reported.[58] Taking the binding constant of ethidium to

be 10^7 M^{-1},[57] a K_{app} of approximately 1.1 $\times$ 10^8 M^{-1} can be calculated for the derivatives. This compares with 1.9 $\times$ 10^6 M^{-1} for SPM and 8.9 $\times$ 10^4 M^{-1} for acridine.[58] Thus, tethering SPM to acridine increased considerably the overall DNA binding affinity as expected from the synergistic activity of two ligands with DNA affinity.[30] The length of the tether as well as the nature of the bond connecting the tether to the acridine moiety had no influence on the K_{app}.

Quenching fluorimetric assays with DNA-bound ethidium (at a low [ethidium]:[DNA] molar ratio, e.g., 0.1:1) can be used to distinguish intercalating agents from nonintercalative ligands[59] and also to determine possible base or sequence preferential binding.[60] The fluorescence quenching (Q) values with [poly(dA-dT)]$_2$ are much smaller than expected for the untethered DNA intercalating acridine.[58] The Q values are closer to values reported for nonintercalative minor groove binding ligands such as distamycin A,[60] which are more efficient quenchers of the bound ethidium fluorophore than planar intercalators because of their larger DNA binding site sizes. In addition, the close Q values determined using CT-DNA, [poly(dA-dT)]$_2$, and [poly(dG-dC)]$_2$ show that the acridine conjugates do not exhibit any significant base selectivity, in contrast to the preference for GC- and AT-rich sequences of acridine[58] and spermine,[27] respectively. Altogether, these results indicate that groove binding modes are involved for DNA binding of the SPM–acridine conjugates and that the binding behavior is more directed by the polycationic SPM side chain than by the intercalating chromophore, as already reported for other acridine conjugates with
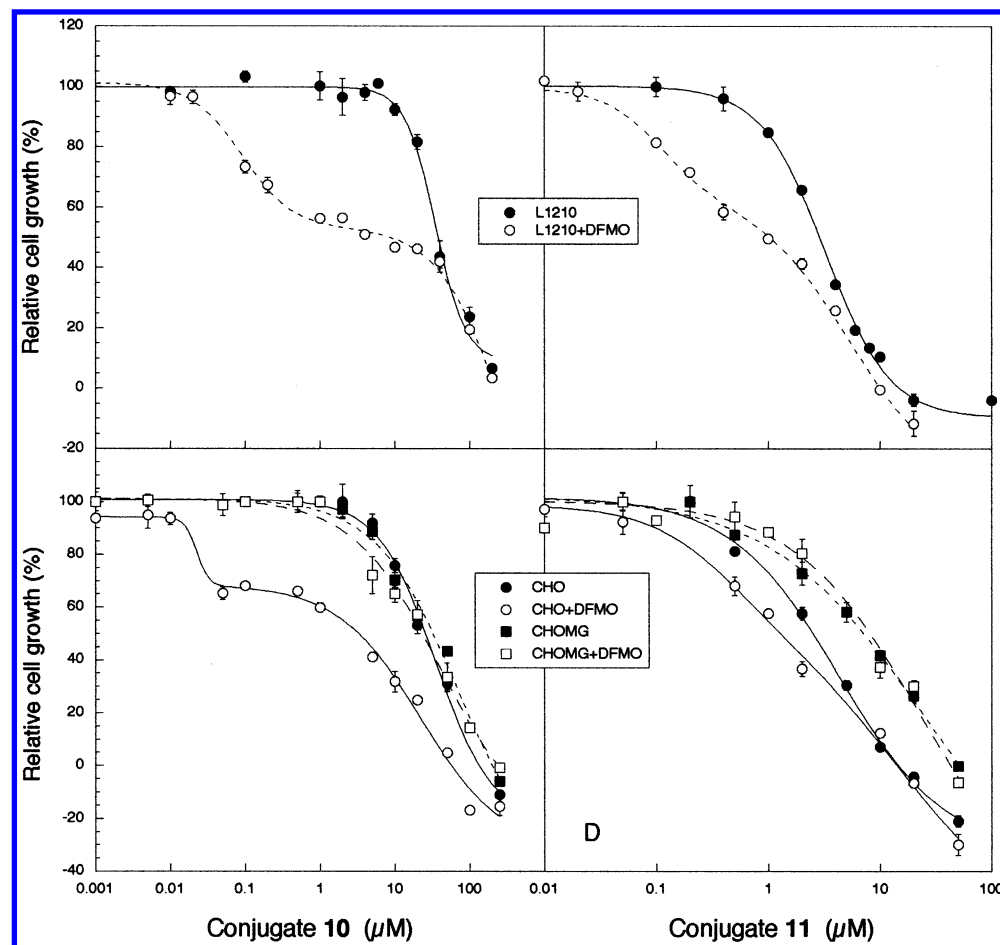
Figure 3. Effect of the conjugates **10** (left panels) and **11** (right panels) on the growth of L1210 (upper panels), CHO, and CHO-MG (lower panels) cells in the presence or absence of DFMO. Cells were treated for 48 h with the conjugates in the presence or absence of 5 mM DFMO. Cell growth rates were determined using an MTT assay. The relative cell growth rates were calculated from the value of cell growth of the corresponding control cells cultured in the absence ($OD_{540\ nm}$ = 0.87, 0.79, and 0.94 for CHO, CHO-MG, and L1210 cells, respectively) or in the presence of DFMO ($OD_{540\ nm}$ = 0.50, 0.45, and 0.55 for CHO, CHO-MG, and L1210 cells, respectively).

functionalized side chains.[58,60,61] This is also consistent with the multiple binding modes observed with our anthracene–polyamine conjugates.[30–32]

3. Growth Inhibitory Effects and Uptake. As with free SPM and other SPM derivatives containing a free terminal primary amine,[62,63] all six acridine conjugates were substrates for bovine serum amine oxidase (data not shown). To prevent cytotoxicity induced by the oxidation products, all experiments were performed in the presence of aminoguanidine (2 mM), an inhibitor of the oxidase. In the presence of micromolar concentrations of the conjugates, the growth rate of L1210 and Chinese hamster ovary (CHO) cells decreased in a concentration-dependent manner. Typical results are shown in Figure 3, and IC_{50} values are listed in Table 2. The architecture of the conjugates clearly modulates their bioactivity, and the nature of the chemical bond linking the amino-aliphatic chain to the acridine moiety has a profound impact on the toxicity of the derivatives. The aminoacridines **11**–**13** (IC_{50} values around 2 μM) were 10–20 times more potent than the amidoacridines **8**–**10** (IC_{50} values between 20 and 40 μM). The length of the spacer showed little influence on the toxicity of the drugs. Qarawi et al.[52] have reported the cytotoxicity on B16 melanoma cells of conjugates composed of a spermine chain conjugated directly to the 9-position of acridine through either an amide (**3**) or an amine (**4**)

Table 2. In Vitro Cell Growth Inhibition[a]

| con-jugate | inhibitory IC_{50}/IC_{25} concn (μM)[c] | | | | | |
| | L1210 | | CHO | | CHO-MG | |
	control	+ DFMO[b]	control	+ DFMO[b]	control	+ DFMO[b]
8	43/22	2.2/0.09	30	nd[d]	35	nd
9	18/10	2.2/0.16	17	nd	21	nd
10	41/22	6.6/0.10	25/10.8	2.0/0.025	31/10.5	23/6.0
11	2.8/1.4	0.9/0.14	2.3/0.9	1.3/0.32	6.1/1.8	7.3/2.5
12	2.3/1.1	0.6/0.16	2.3	nd	7.2	nd
13	1.4/0.4	0.7/0.20	1.0	nd	4.0	nd

[a] All cells were challenged with the conjugates at the time of seeding for L1210 cells and 24 h later for CHO and CHO-MG cells. Cell growth was determined using an MTT assay after 48 h treatment. [b] DFMO (5 mM) was added at the time of the addition of the conjugates. [c] Conjugate concentration required to inhibit cell growth by 50 or 25% after 48 h; mean value (±10%) from three determinations. [d] nd, not determined.

bond. The aminoacridine **4** was more toxic than the amidoacridine **3**. All of these data demonstrate that in terms of cell growth effects, aminoacridines are more favorable than amidoacridines. The positively charged amino group on the 9-position of the aminoacridines is likely to be a critical feature. The site of conjugation on the spermine chain has also a profound impact on the activity of the conjugates in terms of toxicity. Conjugation on the terminal amino group is more beneficial than

Table 3. Inhibition of [^{14}C]SPD Uptake and Cellular Uptake of the Acridine Conjugates in L1210 Cells

| | | cellular uptake in L1210 (nmol/mg protein)[b] | | | | | |
compd	inhibition of [^{14}C]SPD uptake, K_i (μM)[a]	concn (μM)	control	500 μM SPD[c]	Δ[d]	pretreated with 5 mM DFMO[e]	ratio ± DFMO
SPM **1**	1.34						
8	0.097	10	0.239	0.221	0.018	0.587	2.4
		5	0.086	0.073	0.013	nd	
9	0.083	10	0.561	nd		0.850	1.5
10	0.097	10	0.279	0.262	0.017	0.631	2.3
		2	0.064	0.049	0.015	0.217	3.4
		0.5	0.033	0.016	0.017	0.113	3.4
11	0.129	2	0.717	0.553	0.136	1.583	2.2
		1	0.307	0.188	0.119	0.728	2.4
		0.5	0.186	0.053	0.133	0.496	2.7
12	0.083	2	0.491	nd		1.528	3.1
		1	0.362	0.280	0.082	nd	
		0.5	0.193	0.094	0.099	nd	
13	0.135	2	0.510	nd	nd	1.063	2.1

[a] K_i values were determined using multiple concentrations of [^{14}C]SPD in 5 min initial rate transport assays. [b] L1210 cells were cultured for 24 h with the compounds; intracellular levels of the acridine conjugates were determined by fluorimetry; mean value (±15%) from three determinations; nd, not determined. [c] L1210 cells were incubated with the conjugates in the presence of 500 μM SPD. [d] Differential accumulation between control and SPD-treated cells. [e] L1210 cells were pretreated for 24 h with 5 mM DFMO before conjugate addition.

Table 4. Cellular Uptake of the Acridine Conjugates in CHO and CHO-MG Cells

| | | cellular uptake (nmol/mg protein)[a] | | |
conjugate	concn (μM)	CHO	CHO-MG	CHO/CHO-MG
8	10	0.100	0.108	0.93
	2.5	0.014	0.017	0.83
9	10	0.183	0.172	1.1
	1.25	0.018	0.013	1.4
10	10	0.125	0.112	1.1
	2	0.034	0.032	1.1
11	0.5	0.167	0.054	3.1
12	0.5	0.081	0.026	3.1
13	0.5	0.210	0.061	3.4

[a] Conjugates were added 24 h after seeding; intracellular levels of the conjugates were determined by fluorimetry in cells treated with the conjugates during 24 h; mean value (±15%) from three determinations.

on the secondary amino group: the N^1 spermine conjugate **13** (IC$_{50}$ = 1.4 μM) is 16 times more active on L1210 cells than **6**, its N^4 homologue[33] (IC$_{50}$ = 23 μM). All conjugates were also more toxic than unsubstituted acridine (IC$_{50}$ = 45 μM),[58] but **7**, the nonpolyamine-containing 9-(N-butyl)aminoacridine (IC$_{50}$ = 2 μM),[33] was as potent as its spermine-containing homologue **12**.

To check whether the differential toxicity of the two families of acridine conjugates is due to their cellular uptake, we measured the cellular conjugate concentrations in L1210 and CHO cells after 24 h. Conjugates **8**−**13** were taken up by the cells in a dose-dependent manner (Tables 3 and 4, Figure 4). The aminoacridines **11**−**13** were more readily taken up than the amidoacridines **8**−**10**. At concentrations of 10 μM, the intracellular concentrations of **8**−**10** in L1210 cells were at best equivalent to those measured in cells treated with 2 μM **11**−**13**. Moreover, L1210 and CHO cells treated with **9**, the more potent of the three amidoacridines, had significantly higher intracellular concentrations of the conjugate. Thus, the differential activity of the two families of acridine conjugates is at least related to their differential accumulation in the cells.

4. Interaction with the PTS. To determine whether the intracellular accumulation of the conjugates was dependent on the PTS, we determined (i) the ability of the conjugates to compete with [^{14}C]SPD for uptake in

L1210 and CHO cells, (ii) the effect of an excess of free SPD on the accumulation of conjugates in L1210 cells, (iii) the relative growth inhibitory effect and accumulation of the conjugates in CHO and polyamine transport deficient CHO-MG cells, and (iv) the effect of DFMO on the growth inhibitory effect and the uptake of the conjugates.

(i) All six acridine conjugates competitively inhibited the transport of [^{14}C]SPD in L1210 cells with K_i values around 0.1 μM (Table 3). In both series, the lowest K_i value was observed with the conjugates tethered with four methylene units (**9** and **12**). Noteworthy, all derivatives had K_i values approximatively 10 times lower than SPM itself. The coupling of a hydrophobic heterocyclic or aromatic moiety to SPM **1** may improve its affinity for the polyamine transporter. Conjugates **10** and **11** also inhibited the uptake of [^{14}C]SPD in CHO cells in a dose-dependent manner with IC$_{50}$ values of 37 and 60 nM, respectively (Figure 5). Altogether, these data demonstrate that the spermine−acridine conjugates have a high affinity for the PTS.

(ii) Taking into account the affinity of the acridine conjugates deduced from the K_i values (Table 3), 500 μM SPD would inhibit almost completely the uptake of the conjugates via the PTS in L1210 cells. As shown in Table 3, the presence of SPD in the culture medium reduced only partially the amount of conjugates taken up by the cells. In the range of concentrations studied, an excess of SPD reduced cellular uptake by a similar amount (around 0.015 and 0.100 nmol/mg for amido- and aminoacridines, respectively). These amounts are likely to reflect the actual quantity of conjugates that entered the cells via the PTS. These data demonstrate that the amount of conjugates transiting through the PTS is relatively small and that the uptake rate through the PTS is higher for the aminoacridines.

(iii) While conjugates **8**−**10** had similar growth inhibitory effects on CHO and CHO-MG, conjugates **11**−**13** were 3−4 times more active on CHO than CHO-MG cells (Table 2; Figure 3). These effects were correlated with the amount of derivatives accumulated in the cells: CHO and CHO-MG cells accumulated similar amounts of amidoacridines (**8**−**10**) while intracellular concentra-
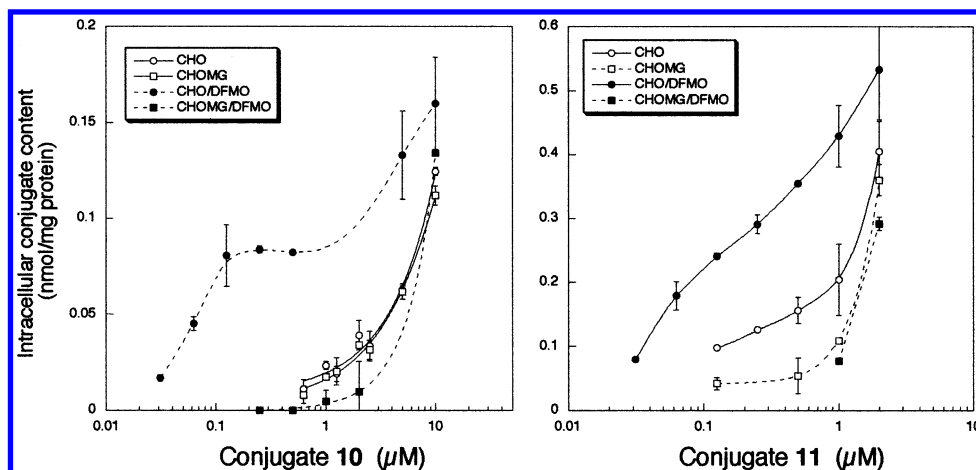
Figure 4. Cellular uptake of the conjugates **10** and **11** in control or DFMO-pretreated CHO and mutant polyamine transport deficient CHO-MG cells. Cells pretreated or not for 24 h with 5 mM DFMO were exposed for 24 h to the conjugates. Intracellular concentrations of the conjugates were determined by fluorimetry.
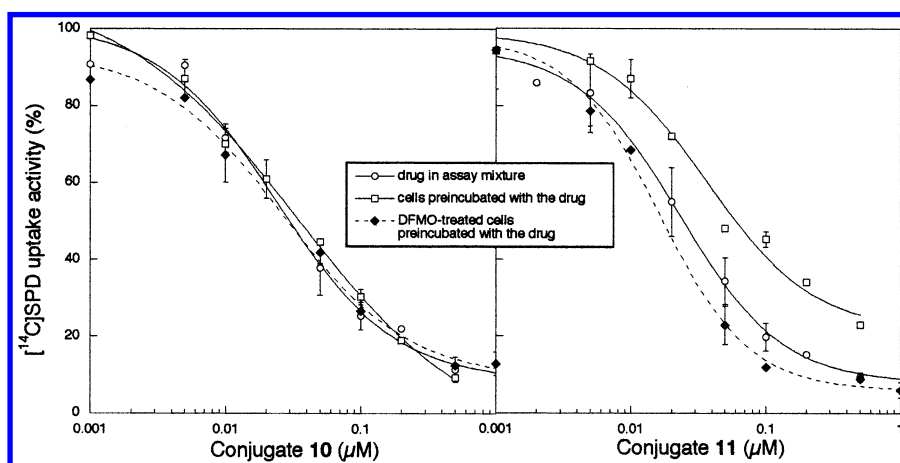

Figure 5. Effect of short term exposure to the conjugates **10** and **11** on the polyamine transport activity in control or DFMO-pretreated CHO cells. CHO cells grown for 24 h with or without 5 mM DFMO were exposed for 2 h to various concentrations of the conjugates. [^{14}C]SPD uptake activity was measured after conjugate removal and washings. The [^{14}C]SPD transport activities in control and DFMO-pretreated cells were 0.29 ± 0.01 and 0.41 ± 0.03 nmol/mg/min, respectively.

tions of aminoacridines (**11**−**13**) were significantly higher (approximately 3-fold) in CHO than in CHO-MG cells (Table 4; Figure 4).

Altogether, these results strongly suggest that the uptake of the acridine conjugates is not solely dependent on the polyamine transport apparatus. The contribution of the PTS to the overall accumulation is more important for aminoacridines than for their amide analogues but still relatively poor. As a comparison, the sensitivity of CHO cells to bis(7-amino-4-azaheptyl)dimethylsilane, a polyamine analogue taken up by the polyamine transporter, was higher by several orders of magnitude than the mutant cell line CHO-MG.[64] The architecture of the derivatives influences both the polyamine transporter-dependent and -independent uptake with a marked preference for the aminoacridines.

(iv) Treatment of L1210, CHO, and CHO-MG cells with DFMO, an inhibitor of ornithine decarboxylase, results in a depletion of intracellular pools of putrescine and SPD. This reduction of intracellular polyamine levels induced an up-regulation of the activity of the PTS in L1210 and CHO cells.[65,66] Exposure of L1210 or CHO cells to the acridine derivatives in the presence of 5mM DFMO enhanced their growth inhibitory activity. Typical examples of dose-dependent growth inhibitory

curves in the presence of DFMO are shown in Figure 3. For the amidoacridines **8**−**10**, the curves were biphasic and showed a strong synergistic effect at low concentrations (Figure 3). Consequently, DFMO decreased more dramatically the IC$_{25}$ than the IC$_{50}$ values. As shown in Table 2, in the presence of DFMO, IC$_{50}$ values for conjugates **8**−**10** were 6−19 times lower while their IC$_{25}$ values were 100−240 times lower. The effect of DFMO on the aminoacridines **11**−**13** was less dramatic (Figure 3; Table 2). DFMO reduced the IC$_{50}$ values by a factor of 2−3 and the IC$_{25}$ values by a factor of 2−10 (Table 2). In contrast, DFMO had no effect on the toxicity of the drugs on CHO-MG cells, which demonstrates that the synergistic effect observed with DFMO is strictly dependent on the presence of an active PTS.

Pretreatment of L1210 or CHO cells with 5 mM DFMO for 24 h increased the uptake of the acridine derivatives but was ineffective in CHO-MG cells (Table 3; Figure 4). Intracellular accumulation of the acridine conjugates was enhanced 2−3 times in DFMO-pretreated L1210 cells when compared to controls. The dose-dependent accumulation of the conjugates **10** and **11** in CHO and CHO-MG cells pretreated with DFMO was studied over a large concentration range. While DFMO had no effect on the accumulation of both

conjugates in CHO-MG, their accumulation was improved in CHO cells as observed in L1210 cells. A remarkable increase was observed with the amidoacridine **10** at concentrations below 0.5 μM, a concentration for which accumulation of the conjugate is below detection level in control cells.

Altogether, from the DFMO studies, we conclude that all these derivatives are able to use the PTS in addition to another independent transport mechanism. The effect of the derivatives on cell growth is dependent on their intracellular concentration, and the effect of DFMO on the cytotoxicity is tentatively explained as follows. For the amidoacridines, the amount of drug transiting through the PTS in normal cells is likely to be too low to exert a cytotoxic effect and the observed toxicity is solely due to the drug penetrating through a polyamine transport-independent system. In contrast, in cells treated with DFMO, the amount of drug taken up by the activated system passes the threshold beyond which a cytotoxic effect can be exerted. Because of the high affinity of the drug for the PTS, these effects are observed at low concentrations. However, for concentrations over 0.1 μM, intracellular concentrations (as well as the effect on cell growth) plateaued. The combined effects of the drugs taken up by the two uptake mechanisms will give an overall dose-dependent biphasic effect. The plateau may be the consequence either of a saturation of the transport system or of a down-regulation of the system preventing higher amounts of drugs being taken up as discussed below. In contrast, higher amounts of aminoacridines transit through the PTS and the threshold is already reached in normal cells. DFMO improves their effect on cell growth in proportion to the amount of drug taken up by the activated transport system.

Because of the high velocity of the PTS, this system would allow a significant accumulation of spermine conjugates in cells. However, the activity of the PTS is highly regulated. In particular, the activity of the PTS is repressed in response to elevated intracellular levels of natural polyamines via the induction of antizyme.[22,67] Feedback control of uptake can also be mimicked by structural analogues of polyamines,[68,69] which indicates that analogues may inhibit their own uptake. In a recent paper, Weeks et al.[70] have shown that the treatment of cells for a short period with a lysine−SPM conjugate, a potent competitive inhibitor of polyamine transport, results in a dose-dependent, antizyme-independent repression of the polyamine transport activity. An immediate increase in transport was observed upon removal of the lysine−SPM conjugate, but the recovery of a full transport activity required several hours of culture in the absence of any polyamine conjugates.[70] When CHO cells were cultured for 2 h with various concentrations of **10** and **11**, the activity of the PTS, measured in a 5 min assay after removal of the conjugates, was inhibited in a dose-dependent manner with IC$_{50}$ values around 25 nM (Figure 5). This inhibitory effect was independent of the initial activity of the PTS as evidenced by the similar inhibition rates determined on DFMO-pretreated cells. These results demonstrate that acridine−spermine conjugates induce a repression of the transport activity in CHO cells. A role for antizyme in this process is excluded because similar inhibition rates were obtained when the conjugates were applied in the presence of 200 μM cycloheximide (data not shown). Following from the potent dose-dependent inhibitory activity of the acridine−spermine conjugates, observed when the conjugates were present in the assay medium, we conclude that the acridine conjugates bind very rapidly and avidly to the transporter. A slow rate of dissociation of the conjugate from the transporter, as hypothesized by Weeks et al.,[70] would prevent the recovery of a full transport activity after removal of the conjugates. Another potential mechanism may involve an interaction with calmodulin. Calmodulin antagonists inhibit polyamine uptake,[71−73] and conjugates of spermine with lipophilic substituents, such as N^1-dansylspermine and N^1-(n-octanesulfonyl)spermine, potent calmodulin antagonists.[62] The exact mechanism of the inhibition of the PTS by the acridine conjugates remains to be fully investigated. It appears obvious from these observations that the repression of the activity of the PTS induced by the acridine conjugates limits their own accumulation via the polyamine transporter and accounts for the low amounts of drugs transiting through the PTS.

Conclusions

Polyamine vectorization is believed to be a valuable strategy to increase the selectivity of anti-cancer agents. However, little is known on the feasibility of this approach in terms of drug delivery. The acridine−spermine conjugates were designed as test compounds to study the influence of polyamine conjugation on cytotoxicity and on the interactions with the PTS.

Our data demonstrate that the concept of polyamine vectorization will successfully depend on the relative amount of drug carried by the specific transporter or using other entry pathways. A selectivity will be reached (i) if the affinity of the drug for the PTS is higher than for other transport system(s) and (ii) if the amount of drug carried by the specific transporter is sufficient to pass the threshold required for the desired biological activity. It is however expected that the tumor selectivity of drugs vectorized by polyamines will need the cotreatment with DFMO to up-regulate the PTS activity of the tumor cells. In this regard, it is important to note that despite the fact that the spermine conjugates **11**−**13** were as potent as their nonpolyamine-containing homologue **7** in normal cells, DFMO has a synergistic effect on the toxicity of conjugates **11**−**13**, an effect dependent on the presence of an active PTS. Such an effect is not anticipated for conjugate **7** because it is certainly not transported by the PTS.

However, the benefits expected from the vectorization by spermine may be diminished by the ability of the conjugates to repress the activity of the PTS of the target cells and therefore to inhibit their own transport. This effect limits the amount of drug transported selectively into the cells. The elucidation of the mechanism of this transport inhibition is under investigation. Our future studies will focus on the design of polyamine conjugates devoid of this disadvantageous property. Modifications of the spermine chain may be a promising approach because in another series of polyamine conjugates, we observed that the substitution of spermine
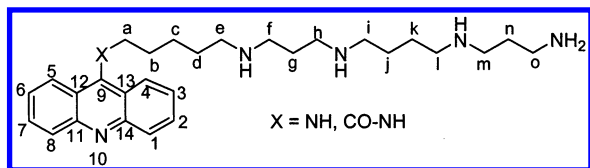
Figure 6. Example of atom numbering used for NMR assignments.

with some synthetic homologous chain reduced the ability of the conjugates to repress the activity of the PTS without altering their affinity for the transporter (unpublished data).

Experimental Section

Reagent-grade solvents were purchased from chemical companies and used directly without further purification unless otherwise specified. Dichloromethane (CH_2Cl_2) was distilled over P_2O_5 under nitrogen. Methanol (MeOH) was distilled over Mg and I_2 prior to use. Elemental analyses were performed by the Laboratoire de Microanalyses (Faculté de Pharmacie, Université Paris XI, Chatenay-Malabry, France). Purifications by column chromatography were carried out over 70−230 mesh silica gel (Merck) using various eluants as specified in the text. Thin-layer chromatography (TLC) was routinely carried out with aluminum sheets precoated with silica gel 60 F254 (layer thickness: 0.22 mm) (Merck). Solvent systems (expressed in volume percents) and R_f are indicated in the text. The compounds were visualized under UV light and staining with $KMnO_4$, anisaldehyde, or ninhydrin. Fourier transform IR (FTIR) spectra were recorded on a Perkin-Elmer 377 instrument (KBr pellets, ν: cm^{-1}). NMR spectra were recorded on a Bruker DMX spectrometer at 500 MHz (^{1}H) or 125 MHz (^{13}C), on a JEOL EX400 spectrometer at 400 MHz (^{1}H) or 100 MHz (^{13}C), or on a JEOL GX270 spectrometer at 270 MHz (^{1}H) or 68 MHz (^{13}C). Tetramethylsilane (TMS) was used as the internal standard for NMR spectra recorded in CDCl$_3$. 3-(Trimethylsilyl)-1-propanesulfonic acid sodium salt (DSS) was used as the external standard for NMR spectra recorded in D_2O. Broad band and gated decoupling ^{13}C NMR spectra were recorded, and the assignments were made using chemical shifts and coupling constants. High-resolution mass spectra (HRMS), determined by liquid secondary-ion mass spectrometry (LSIMS), were recorded on a ZabSpec Tof Micromass instrument (Centre Régional de Mesures Physiques de l'Ouest, Rennes, France) with a source temperature of 140 °C, an ion (Cs$^+$) accelerating potential of 8 kV, and mNBA (*meta*-nitrobenzyl alcohol) as the matrix. Low-resolution mass spectra (LRMS) were determined by chemical ionization (MS-CI) or by fast atomic bombardment (MS-FAB) recorded on a VG autospec. As indicated in Figure 6, the compounds were numbered for the heterocyclic moiety using the IUPAC rules and for the polyamine moiety with letters a−o.

1. Chemical Syntheses. General Procedure for Amino Alcohol Synthesis under Schotten−Bauman Conditions. The amino alcohol (3-aminopropan-1-ol, 4-aminobutan-1-ol, or 5-aminopentan-1-ol, 2 g) was dissolved at 0 °C in aqueous NaOH (1.1 equiv). Benzylchloroformate (1.1 equiv) was added dropwise. The reaction mixture was allowed to warm to room temperature and stirred overnight. After the solvents were evaporated under reduced pressure, the residue was purified. TLC was performed in 200/10/1 CH_2Cl_2/MeOH/NH$_4$OH and visualized using $KMnO_4$.

Data for *N*-Benzyloxycarbonyl-3-aminopropan-1-ol (14). Compound **14** was prepared from 3-aminopropan-1-ol and benzylchloroformate; purified by column chromatography (200/10/1 CH_2Cl_2/MeOH/NH$_4$OH); white solid; 97%; R_f 0.30. ^{1}H NMR (270 MHz, CDCl$_3$): δ 1.69 (m, 2H, CH$_2$C*H$_2$*CH$_2$), 2.03 and 2.95 (br s, 1H, OH), 3.30−3.37 (m, 2H, C*H$_2$*NH), 3.66 (m, 2H, C*H$_2$*OH), 5.09 (s, 2H, OC*H$_2$*C$_6$H$_5$), 7.30−7.34 (m, 5H, H−Ar). ^{13}C NMR (68 MHz, CDCl$_3$): δ 32.43 (CH$_2$*C*H$_2$CH$_2$), 37.69 (*C*H$_2$NH), 59.47 (*C*H$_2$OH), 66.78 (O*C*H$_2$C$_6$H$_5$), 128.02,

128.10, 128.48 (*C*H−Ar), 136.37 (OCH$_2$*C*C$_5$H$_5$), 157.29 (C=O). MS-FAB (*m/z*) calcd for C$_{11}$H$_{16}$NO$_3$ (M + H), 210.25; found, 210.20.

Data from *N*-Benzyloxycarbonyl-4-aminobutan-1-ol (15). Compound **15** was prepared from 4-aminobutan-1-ol and benzylchloroformate; purified by recrystallization with AcOEt/hexane; white solid; 90%; R_f 0.34. ^{1}H NMR (270 MHz, CDCl$_3$): δ 1.57 (m, 4H, CH$_2$C*H$_2$*C*H$_2$*CH$_2$), 2.02 and 2.39 (br s, 1H, OH), 3.20 (m, 2H, C*H$_2$*NH), 3.63 (m, 2H, C*H$_2$*OH), 5.08 (s, 2H, OC*H$_2$*C$_6$H$_5$), 7.26−7.34 (m, 5H, H−Ar). ^{13}C NMR (68 MHz, CDCl$_3$): δ 26.41 and 29.55 (CH$_2$*C*H$_2$*C*H$_2$CH$_2$), 40.74 (*C*H$_2$NH), 62.19 (*C*H$_2$OH), 66.56 (O*C*H$_2$C$_6$H$_5$), 128.02, 128.44 (*C*H−Ar), 136.54 (OCH$_2$*C*C$_5$H$_5$), 156.55 (C=O). MS-FAB (*m/z*) calcd for C$_{12}$H$_{18}$NO$_3$ (M + H), 224.27; found, 224.20.

Data from *N*-Benzyloxycarbonyl-5-aminopentan-1-ol (16). Compound **16** was prepared from 5-aminopentan-1-ol and benzylchloroformate; purified by recrystallization with AcOEt/hexane; white solid; 84%; R_f 0.43. ^{1}H NMR (270 MHz, CDCl$_3$): δ 1.35−1.43 and 1.47−1.62 (m, 6H, CH$_2$C*H$_2$*C*H$_2$*C*H$_2$*CH$_2$), 1.84 (br s, 1H, OH), 3.20 (m, 2H, C*H$_2$*NH), 3.62 (t, 2H, J = 6.2 Hz, C*H$_2$*OH,), 5.08 (s, 2H, OC*H$_2$*C$_6$H$_5$), 7.26−7.36 (m, 5H, H−Ar). ^{13}C NMR (68 MHz, CDCl$_3$): δ 22.82, 26.67 and 32.14 (CH$_2$*C*H$_2$*C*H$_2$*C*H$_2$CH$_2$), 40.87 (*C*H$_2$NH), 62.52 (*C*H$_2$OH), 66.56 (O*C*H$_2$C$_6$H$_5$), 128.04, 128.46 (*C*H−Ar), 136.57 (OCH$_2$-*C*C$_5$H$_5$), 156.48 (C=O). MS-FAB (*m/z*) calcd for C$_{13}$H$_{20}$NO$_3$ (M + H), 238.30; found, 238.20.

General Procedure of Swern Oxidation. Oxalyl chloride (1.1 equiv) was dissolved in 15 mL of anhydrous CH_2Cl_2 and cooled to −78 °C (ice dry and acetone). Anhydrous dimethyl sulfoxide (DMSO, 2 equiv) was then added dropwise over 5 min using a syringe, and the reaction mixture was stirred at −78 °C for 10 min. *N*-Benzyloxycarbonyl-amino alcohol (1 equiv) dissolved in CH_2Cl_2 (35 mL) was added dropwise over 5 min, and a yellow precipitate was formed. The reaction mixture was then warmed until the precipitate dissolved. The reaction mixture was cooled to −78 °C and stirred for 10 min. Et$_3$N (5 equiv) was then added, the reaction was warmed to room temperature, and water (50 mL) was added. After the organic layer was separated, the aqueous layer was extracted with CH_2Cl_2 (2 × 50 mL), the combined organic layers were dried with MgSO$_4$, and then, the solvents were evaporated under reduced pressure. The residue was purified by column chromatography in AcOEt/hexane 40/60 and then 50/50. TLC was performed in AcOEt/hexane 40/60 and visualized using anisaldehyde.

Data for *N*-Benzyloxycarbonyl-3-aminopropanal (17). Compound **17** was prepared from **14**; white solid; 50%; R_f 0.32. ^{1}H NMR (270 MHz, CDCl$_3$): δ 2.74 (t, 2H, J = 5.8 Hz, C*H$_2$*CHO), 3.49 (m, 2H, C*H$_2$*NH), 5.08 (s, 2H, OC*H$_2$*C$_6$H$_5$), 7.26−7.34 (m, 5H, H−Ar), 9.79 (s, 1H, C*H*O). ^{13}C NMR (100 MHz, CDCl$_3$): δ 34.47 (*C*H$_2$NH), 44.09 (*C*H$_2$CHO), 66.77 (O*C*H$_2$C$_6$H$_5$), 128.11, 128.18, 128.55 (*C*H−Ar), 136.37 (OCH$_2$-*C*C$_5$H$_5$), 156.31 (C=O), 201.22 (CHO). MS-FAB (*m/z*) calcd for C$_{11}$H$_{14}$NO$_3$ (M + H), 208.23; found, 208.10.

Data for *N*-Benzyloxycarbonyl-2-hydroxypyrrolidine (18). Compound **18** was prepared from **15**; yellow solid; 87%; R_f 0.34. ^{1}H NMR (270 MHz, CDCl$_3$, mixture of conformational isomers): δ 1.86−2.04 (m, 4H, NCH$_2$C*H$_2$*C*H$_2$*CHOH), 3.13 and 3.95 (br s, 1H, OH), 3.36 (m, 1H, NC*H$_2$*), 3.58 (m, 1H, NC*H$_2$*), 5.17 (s, 2H, OC*H$_2$*C$_6$H$_5$), 5.48−5.54 (m, 1H, OHC*H*N), 7.26−7.37 (m, 5H, H−Ar). ^{13}C NMR (100 MHz, CDCl$_3$, mixture of conformational isomers): δ 22.05 and 22.79 (NCH$_2$*C*H$_2$CH$_2$-CHOH), 32.66 and 33.58 (NCH$_2$CH$_2$*C*H$_2$CHOH), 45.78 and 46.23 (N*C*H$_2$), 66.90 and 67.14 (O*C*H$_2$C$_6$H$_5$), 81.21 and 82.00 (OH*C*HN), 127.87, 128.09, 128.29, 128.53 and 128.66 (*C*H−Ar), 136.37 and 136.47 (OCH$_2$*C*C$_5$H$_5$), 154.15 and 155.50 (C=O). [74] MS-CI (*m/z*) calcd for C$_{12}$H$_{16}$NO$_3$ (M + H), 222.26; found, 222.10.

Data for *N*-Benzyloxycarbonyl-2-hydroxypiperidine (19). Compound **19** was prepared from **16**; white solid; 73%; R_f 0.47. ^{1}H NMR (270 MHz, CDCl$_3$, mixture of conformational isomers): δ 1.81−2.10 (m, 6H, NCH$_2$C*H$_2$*C*H$_2$*C*H$_2$*CHOH), 3.07 and 3.95 (br s, 1H, OH), 3.35 (m, 1H, NC*H$_2$*), 3.59 (m, 1H, NC*H$_2$*), 5.14 (s, 2H, OC*H$_2$*C$_6$H$_5$), 5.49−5.54 (m, 1H, OHC*H*N),

7.27–7.37 (m, 5H, H–Ar). ^{13}C NMR (68 MHz, CDCl$_3$, mixture of conformational isomers): δ 21.99 and 22.72 (NCH$_2$*C*H$_2$*C*H$_2$-CH$_2$CHOH), 32.62 and 33.54 (NCH$_2$CH$_2$CH$_2$*C*H$_2$CHOH), 45.71 and 46.17 (N*C*H$_2$), 66.85 and 67.08 (O*C*H$_2$C$_6$H$_5$), 81.14 and 81.91 (OH*C*HN), 127.81, 128.02, 128.22, 128.46 and 128.59 (*C*H–Ar), 136.31 and 136.42 (OCH$_2$*C*C$_5$H$_5$), 153.51 and 154.35 (*C*=O). MS-CI (*m/z*) calcd for C$_{13}$H$_{18}$NO$_3$ (M + H), 236.29; found, 236.10.

Procedure for N^1,N^4,N^9-Tri-*tert*-butoxycarbonylspermine Synthesis (20). Compound **20** was made as previously described;[49] 44%; R_f 0.38 (CH$_2$Cl$_2$/MeOH/NH$_4$OH 70/10/1 and visualized using ninhydrin). ^{1}H NMR (400 MHz, CDCl$_3$): δ 1.28–1.48 (m, 31H, 3(C*H$_3$*)$_3$C, H-6, H-7), 1.59–1.66 (m, 4H, H-2, H-11), 2.74 (m, 2H, H-12), 3.00–3.45 (m, 12H, H-1, H-3, H-5, H-8, H-10, NH$_2$). ^{13}C NMR (100 MHz, CDCl$_3$): δ 25.42 and 26.02 (C-6, C-7), 28.09 and 28.93 (3(*C*H$_3$)$_3$C, C-2), 30.15 and 32.30 (C-11), 37.36 and 37.71 (C-1), 38.35 and 39.35 (C-12), 43.54 and 44.42 (C-3, C-10), 46.43 and 46.82 (C-5, C-8), 78.96 and 79.74 ((CH$_3$)$_3$*C*), 155.52 and 156.21 (C=O).

General Method of Reductive Amination. Compound **17**, **18**, or **19** (1 equiv) was dissolved with **20** (1.4 equiv) in anhydrous MeOH (10 mL), and the solution was stirred on molecular sieves 4 Å under N$_2$ at 25 °C. Sodium cyanoborohydride (1.7 equiv) and a catalytic amount of glacial acetic acid (0.1 mL) were then added, and the reaction mixture was stirred at 25 °C for 24 (for **17**), 48 (for **18**), or 72 h (for **19**). The mixture was then filtered and concentrated under reduced pressure. The residue was then chromatographed in CH$_2$Cl$_2$/MeOH/NH$_4$OH 100/10/1. TLC was performed in CH$_2$Cl$_2$/MeOH/NH$_4$OH 100/10/1 and visualized using ninhydrin.

Data for N^1,N^5,N^{10}-Tri-*tert*-butoxycarbonyl-N^{18}-benzyloxycarbonyl-1,5,10,14,18-pentaazaoctadecane (21). Compound **21** was prepared from **17**; yellow oil; 54%; R_f 0.34. ^{1}H NMR (400 MHz, CDCl$_3$): δ 1.44–1.45 (m, 31H, 3(C*H$_3$*)$_3$C, H-7, H-8), 1.69 (m, 6H, H-3, H-12, H-16), 2.07 (br s, 1H, NH), 2.56–2.69 (m, 4H, H-13, H-15), 3.13–3.48 (m, 12H, H-2, H-4, H-6, H-9, H-11, H-17), 5.09 (s, 2H, OC*H$_2$*C$_6$H$_5$), 7.30–7.36 (m, 5H, H–Ar). MS-FAB (*m/z*) calcd for C$_{36}$H$_{64}$N$_5$O$_8$ (M + H), 694.93; found, 694.30.

Data for N^1,N^5,N^{10}-Tri-*tert*-butoxycarbonyl-N^{19}-benzyloxycarbonyl-1,5,10,14,19-pentaazanonadecane (22). Compound **22** was prepared from **18**; colorless oil; 40%; R_f 0.36. ^{1}H NMR (500 MHz, CDCl$_3$): δ 1.44–2.00 (m, 40H, 3(C*H$_3$*)$_3$C, H-3, H-7, H-8, H-12, H-16, H-17, NH), 2.56–2.89 (m, 4H, H-13, H-15), 3.10–3.33 (m, 12H, H-2, H-4, H-6, H-9, H-11, H-18), 5.09 (s, 2H, OC*H$_2$*C$_6$H$_5$), 7.30–7.33 (m, 5H, H–Ar). MS-FAB (*m/z*) calcd for C$_{37}$H$_{66}$N$_5$O$_8$ (M + H), 708.95; found, 708.30.

Data for N^1,N^5,N^{10}-Tri-*tert*-butoxycarbonyl-N^{20}-benzyloxycarbonyl-1,5,10,14,20-pentaazaeicosane (23). Compound **23** was prepared from **19**; yellow oil; 29%; R_f 0.16. ^{1}H NMR (500 MHz, CDCl$_3$): δ 1.23–2.06 (m, 42H, 3(C*H$_3$*)$_3$C, H-3, H-7, H-8, H-12, H-16, H-17, H-18, NH), 2.78–2.92 (m, 4H, H-13, H-15), 3.10–3.58 (m, 12H, H-2, H-4, H-6, H-9, H-11, H-19), 5.09 (s, 2H, OC*H$_2$*C$_6$H$_5$), 7.30–7.36 (m, 5H, H–Ar).

General Procedure of TetraBoc Pentamine Formation. To a solution of **21**, **22**, or **23** (1 equiv) in dimethylformamide (DMF, 5 mL), di-*tert*-butyl dicarbonate (1.2 equiv) dissolved in 1 mL of DMF was added at 0 °C under N$_2$. The reaction mixture was stirred at room temperature for 1 h. Concentrated NH$_4$OH (1 mL) was added, and the reaction mixture was stirred for 20 min. The solvents were evaporated under reduced pressure at 40 °C. Pearlman's catalyst (1 equiv) was then added to the residue dissolved in 3 mL of MeOH. The mixture was stirred for 4 h under an atmosphere of H$_2$ at 25 °C. The mixture was filtered, washed with MeOH, and concentrated under reduced pressure. The residue was purified by column chromatography in CH$_2$Cl$_2$/MeOH/NH$_4$OH 100/10/1. TLC was performed in CH$_2$Cl$_2$/MeOH/NH$_4$OH 100/10/1 and visualized using ninhydrin.

Data for N^1,N^5,N^{10},N^{14}-Tetra-*tert*-butoxycarbonyl-1,5,10,14,18-pentaazaoctadecane (24). Compound **24** was prepared from **21**; colorless oil; 63%; R_f 0.10. ^{1}H NMR (400 MHz, CDCl$_3$): 1.44–1.45 (m, 40H, 4(C*H$_3$*)$_3$C, H-7, H-8), 1.66–1.75 (m, 6H, H-3, H-12, H-16), 1.99 (br s, 2H, NH$_2$), 2.85 (m,

2H, H-17), 3.16–3.64 (m, 14H, H-2, H-4, H-6, H-9, H-11, H-13, H-15). MS-FAB (*m/z*) calcd for C$_{33}$H$_{66}$N$_5$O$_8$ (M + H), 660.91; found, 660.30.

Data for N^1,N^5,N^{10},N^{14}-Tetra-*tert*-butoxycarbonyl-1,5,10,14,19-pentaazanonadecane (25). Compound **25** was prepared from **22**; colorless oil; 32%; R_f 0.10 (c). ^{1}H NMR (500 MHz, CDCl$_3$): δ 1.25–1.88 (m, 48H, 4(C*H$_3$*)$_3$C, H-3, H-7, H-8, H-12, H-16, H-17), 2.17 (br s, 2H, NH$_2$), 2.90 (m, 2H, H-18), 3.10–3.42 (m, 14H, H-2, H-4, H-6, H-9, H-11, H-13, H-15). MS-FAB (*m/z*) calcd for C$_{34}$H$_{68}$N$_5$O$_8$ (M + H), 674.94; found, 674.30.

Data for N^1,N^5,N^{10},N^{14}-Tetra-*tert*-butoxycarbonyl-1,5,10,14,20-pentaazaeicosane (26). Compound **26** was prepared from **23**; colorless oil; 34%; R_f 0.10. ^{1}H NMR (500 MHz, CDCl$_3$): δ 1.24–1.85 (m, 50H, 4(C*H$_3$*)$_3$C, H-3, H-7, H-8, H-12, H-16, H-17, H-18), 3.02–3.35 (m, 16H, H-2, H-4, H-6, H-9, H-11, H-13, H-15, H-19), 8.13 (br s, 2H, NH$_2$). MS-FAB (*m/z*) calcd for C$_{35}$H$_{70}$N$_5$O$_8$ (M + H), 688.96; found, 688.30.

General Procedure of Acylation. To a solution of **24**–**26** (1 equiv) in DMF (3 mL) was added acridine-9-carboxylic acid (1 equiv). After it was dissolved, *N,N*-dicyclohexylcarbodiimide (1.2 equiv) and then N^1-hydroxybenzotriazole (catalytical amount, 0.01 equiv) were added. The reaction mixture was stirred at room temperature for 48 h. The precipitate was then removed by filtration. The solvents were evaporated under reduced pressure, and the residue was purified by column chromatography in MeOH/NH$_4$OH 95/5. TLC was performed in CH$_2$Cl$_2$/MeOH 95/5 and visualized using ninhydrin (a). The removal of Boc groups was achieved overnight using a 0.9 M solution of HCl gas in AcOEt. TLC was performed in isopropylamine/MeOH/CHCl$_3$ 2/4/4 and visualized using ninhydrin (b).

Data for N^1-(Acridin-9-ylcarbonyl)-1,5,9,14,18-pentaazaoctadecane Pentahydrochloride (8). Boc-protected **27** was prepared from **24** (yellow oil; 64%; R_f 0.26 (a)). Deprotection gave **8** in 93% yield. Yellow solid; R_f 0.06 (b). FTIR 2300–3700 (NH$^+$), 1636 (C=N + C=O). ^{1}H NMR (500 MHz, D$_2$O): δ 1.79–1.83 (m, 4H, H-h, H-i), 2.11 (m, 2H, H-b), 2.15–2.29 (m, 4H, H-e, H-l), 3.10–3.37 (m, 14H, H-c, H-d, H-f, H-g, H-j, H-k, H-m), 3.83 (t, 2H, *J* = 7 Hz, H-a), 7.97 (t, 2H, *J* = 7 Hz, H-3, 6), 8.27–8.31 (m, 4H, H-2, 7 and H-4, 5), 8.38 (d, 2H, *J* = 9 Hz, H-1, 8). ^{13}C NMR (125 MHz, D$_2$O): δ 23.11, 23.16 (C-e, C-h, C-i), 24.13 (C-l), 25.88 (C-b), 36.93 (C-m), 37.83 (C-a), 44.88, 44.93, 45.03 (C-d, C-f, C-k), 46.01 (C-c), 47.23 and 47.39 (C-g, C-j), 120.62 (C-1, 8), 122.70 (C-12, 13), 126.47 (C-4, 5), 129.73 (C-3, 6), 138.07 (C-2, 7), 140.57 (C-11, 14), 150.32 (C-9), 166.83 (C=O). HRMS (LSIMS) (*m/z*) calcd for C$_{27}$H$_{41}$N$_6$O (M + H), 465.3342; found, 465.3347. Anal. (C$_{27}$H$_{40}$N$_6$O·5HCl·3H$_2$O) calcd: C, 46.44; H, 7.36; N, 12.04. Found: C, 45.96; H, 7.63; N, 12.06.

Data for N^1-(Acridin-9-ylcarbonyl)-1,6,10,15,19-pentaazanonadecane Pentahydrochloride (9). Boc-protected **28** was prepared from **25** (yellow oil; 54%; R_f 0.23 (a)). Deprotection gave **9** in 96% yield. Yellow solid; R_f 0.07 (b). FTIR 2300–3700 (NH$^+$), 1638 (C=N + C=O). ^{1}H NMR (500 MHz, D$_2$O): δ 1.80–1.85 (m, 4H, H-i, H-j), 1.91–1.96 (m, 4H, H-b, H-c), 2.10–2.20 (m, 4H, H-f, H-m), 3.10–3.23 (m, 14H, H-e, H-g, H-h, H-k, H-l, H-n), 3.78 (m, 2H, H-a), 7.97 (t, 2H, *J* = 7 Hz, H-3, 6), 8.27–8.30 (m, 4H, H-2, 7 and H-4, 5), 8.38 (d, 2H, *J* = 9 Hz, H-1, 8). ^{13}C NMR (125 MHz, D$_2$O): δ 23.10, 23.16 (C-f, C-i, C-j), 23.79 (C-c), 24.13 (C-m), 25.94 (C-b), 36.94 (C-n), 40.18 (C-a), 44.86, 44.90, 44.93 (C-e, C-g, C-l), 47.40 and 47.42 (C-h, C-k), 47.78 (C-d), 120.32 (C-1, 8), 122.65 (C-12, 13), 126.54 (C-4, 5), 129.76 (C-3, 6), 138.26 (C-2, 7), 140.26 (C-11, 14), 150.91 (C-9), 166.41 (C=O). HRMS (LSIMS) (*m/z*) calcd for C$_{28}$H$_{43}$N$_6$O (M + H), 479.3498; found, 479.3507. Anal. (C$_{28}$H$_{42}$N$_6$O·5HCl·H$_2$O) calcd: C, 49.73; H, 7.30; N, 12.43. Found: C, 50.02; H, 7.57; N, 12.34.

Data for N^1-(Acridin-9-ylcarbonyl)-1,7,11,16,20-pentaazaeicosane Pentahydrochloride (10). Boc-protected **29** was prepared from **26** (yellow oil; 67%; R_f 0.26 (a)). Deprotection gave **10** in 84% yield. Yellow solid; R_f 0.10 (b). FTIR 2300–3700 (NH$^+$), 1638 (C=N + C=O). ^{1}H NMR (500 MHz, D$_2$O): δ 1.59 (m, 2H, H-c), 1.82–1.89 (m, 8H, H-b, H-d, H-j, H-k), 2.10–2.20 (m, 4H, H-g, H-n), 3.12–3.22 (m, 14H, H-e, H-f, H-h,

H-i, H-l, H-m, H-o), 3.72 (t, 2H, $J = 7$ Hz, H-a), 7.89 (m, 2H, H-3, 6), 8.16−8.21 (m, 6H, H-1, 8, H-2, 7 and H-4, 5). ^{13}C NMR (125 MHz, D$_2$O): δ 23.11, 23.16 (C-g, C-j, C-k), 23.81 (C-c), 24.13 (C-n), 25.61 (C-d), 28.23 (C-b), 36.95 (C-o), 40.48 (C-a), 44.79, 44.91, 44.94 (C-f, C-h, C-m), 48.07 (C-e), 47.40 and 47.42 (C-i, C-l), 121.08 (C-1, 8), 122.47 (C-12, 13), 126.31 (C-4, 5), 129.52 (C-3, 6), 137.48 (C-2, 7), 140.94 (C-11, 14), 149.88 (C-9), 166.57 (C=O). HRMS (LSIMS) (*m/z*) calcd for C$_{29}$H$_{45}$N$_6$O (M + H), 493.3655; found, 493.3659. Anal. (C$_{29}$H$_{44}$N$_6$O·5HCl·3H$_2$O) calcd: C, 47.96; H, 7.63; N, 11.57. Found: C, 48.23; H, 7.71; N, 11.41.

General Procedure of Alkylation. Compound **24**, **25**, or **26** (1 equiv) and 9-phenoxyacridine (1 equiv, prepared as previously described)[50−52] was stirred with 5 g of phenol at 80 °C under a nitrogen atmosphere for 5 h. To the resulting mixture were added CH$_2$Cl$_2$ (30 mL) and NaOH 1 N (20 mL). After it was decanted, washed with NaOH 1 N (4 × 20 mL), and dried over K$_2$CO$_3$, the organic layer was evaporated under reduced pressure and then the residue was purified by column chromatography with a mixture of CH$_2$Cl$_2$/MeOH/NH$_4$OH 98/2/0.2 and then 97/3/0.3, 96/4/0.4 and then 95/5/0.5. TLC was performed in CH$_2$Cl$_2$/MeOH/NH$_4$OH 95/5/0.5 and visualized using ninhydrin (c). The removal of Boc groups was achieved using a 0.9 M solution of HCl gas in ethyl acetate (16 h). TLC was performed in isopropylamine/MeOH/CHCl$_3$ 2/4/4 and visualized using ninhydrin (b).

Data for *N^1*-(Acridin-9-yl)-1,5,9,14,18-pentaazaocta-decane Hexahydrochloride (11). Boc-protected **30** was prepared from **24** (yellow oil; 65%; R_f 0.36 (c)). Deprotection gave **11** in 75% yield. Yellow solid; R_f 0.10 (b), 0.15 (MeOH/NH$_4$OH 70/30), 0.35 (MeOH/NH$_4$OH 50/50). FTIR 2300−3700 (NH$^+$), 1634 (C=N). ^{1}H NMR (500 MHz, D$_2$O): δ 1.79−1.85 (m, 4H, H-h, H-i), 2.09−2.20 (m, 4H, H-e, H-l), 2.26 (m, 2H, H-b), 3.12−3.16 (m, 6H, H-g, H-j, H-m), 3.18−3.22 (m, 8H, H-c, H-d, H-f, H-k), 3.93 (t, 2H, $J = 7.5$ Hz, H-a), 7.31 (d, 2H, $J = 9$ Hz, H-1, 8), 7.41 (t, 2H, $J = 8$ Hz, H-3, 6), 7.78 (t, 2H, $J = 7.5$ Hz, H-2, 7), 7.96 (d, 2H, $J = 9$ Hz, H-4, 5). ^{13}C NMR (125 MHz, D$_2$O): δ 23.12, 23.16 (C-e, C-h, C-i), 24.14 (C-l), 26.27 (C-b), 36.93 (C-m), 44.86, 44.94, 45.10 (C-d, C-f, C-k), 45.40 (C-c), 45.89 (C-a), 47.23 and 47.40 (C-g, C-j), 111.78 (C-12, 13), 118.40 (C-1, 8), 124.45 (C-3, 6, C-4, 5), 135.66 (C-2, 7), 138.88 (C-11, 14), 156.96 (C-9). HRMS (LSIMS) (*m/z*) calcd for C$_{26}$H$_{41}$N$_6$ (M + H), 437.3393; found, 437.3400.

Data for *N^1*-(Acridin-9-yl)-1,6,10,15,19-pentaazanona-decane Hexahydrochloride (12). Boc-protected **31** was prepared from **25** (yellow oil; 54%; R_f 0.33 (c)). Deprotection gave **12** in 71% yield. Yellow solid; R_f 0.07 (b). FTIR 2300−3700 (NH$^+$), 1632 (C=N). ^{1}H NMR (500 MHz, D$_2$O): δ 1.80−1.84 (m, 6H, H-c, H-i, H-j), 1.92 (m, 2H, H-b), 2.11−2.17 (m, 4H, H-f, H-m), 3.12−3.20 (m, 14H, H-d, H-e, H-g, H-h, H-k, H-l, H-n), 3.91 (t, 2H, $J = 7$ Hz, H-a), 7.41 (d, 2H, $J = 9$ Hz, H-1, 8), 7.45 (t, 2H, $J = 7.5$ Hz, H-3, 6), 7.84 (t, 2H, $J = 8$ Hz, H-2, 7), 8.04 (d, 2H, $J = 9$ Hz, H-4, 5). ^{13}C NMR (125 MHz, D$_2$O): δ 23.10, 23.15 (C-f, C-i, C-j), 23.38 (C-c), 24.13 (C-m), 26.48 (C-b), 36.93 (C-n), 44.87, 44.93 (C-e, C-g, C-l), 47.67 (C-d), 48.39 (C-a), 47.39 and 47.42 (C-h, C-k), 118.41 (C-1, 8), 124.20 (C-3, 6, C-4, 5), 135.54 (C-2, 7), 157.37 (C-9). HRMS (LSIMS) (*m/z*) calcd for C$_{27}$H$_{43}$N$_6$ (M + H), 451.3549; found, 451.3542.

Data for *N^1*-(Acridin-9-yl)-1,7,11,16,20-pentaazaeicosane Hexahydrochloride (13). Boc-protected **32** was prepared from **26** (yellow oil; 59%; R_f 0.32 (c)). Deprotection gave **13** in 82% yield. Yellow solid; R_f 0.08 (b). FTIR 2300−3700 (NH$^+$), 1632 (C=N). ^{1}H NMR (500 MHz, D$_2$O): δ 1.48 (m, 2H, H-c), 1.73−1.88 (m, 8H, H-b, H-d, H-j, H-k), 2.09−2.17 (m, 4H, H-g, H-n), 3.08−3.20 (m, 14H, H-e, H-f, H-h, H-i, H-l, H-m, H-o), 3.82 (t, 2H, $J = 7.5$ Hz, H-a), 7.37 (d, 2H, $J = 9$ Hz, H-1, 8), 7.41 (t, 2H, $J = 8$ Hz, H-3, 6), 7.80 (t, 2H, $J = 7.5$ Hz, H-2, 7), 7.99 (d, 2H, $J = 9$ Hz, H-4, 5). ^{13}C NMR (125 MHz, D$_2$O): δ 23.10, 23.15 (C-g, C-j, C-k), 23.51 (C-c), 24.13 (C-n), 25.67 (C-d), 28.93 (C-b), 36.95 (C-o), 44.81, 44.89, 44.93 (C-f, C-h, C-m), 48.02 (C-e), 48.79 (C-a), 47.39 et 47.43 (C-i, C-l), 118.34 (C-1, 8), 124.12 (C-3, 6, C-4, 5), 135.48 (C-2, 7), 157.11 (C-9). HRMS (LSIMS) (*m/z*) calcd for C$_{28}$H$_{45}$N$_6$ (M + H), 465.37057; found,

465.3692. Anal. (C$_{28}$H$_{44}$N$_6$·6HCl) calcd: C, 49.44; H, 7.37; N, 12.35. Found: C, 49.13; H, 7.52; N, 12.07.

2. Biological Studies. Unless otherwise stated, usual laboratory chemicals were purchased from Merck (Darmstadt, Germany) or Sigma Chemical Co. (St Louis, MO). DFMO was obtained from ILEX Oncology (San Antonio, TX). Data are given as mean values of three or more experiments. Comparisons between means were made using the Student's *t*-test assuming significance at $p < 0.01$.

a. Visible Absorption and Fluorimetry. Visible absorption spectra were recorded on a Varian DMS 300 spectrophotometer (Les Ulis, France), and the fluorescence excitation and emission spectra were recorded on a Fluorolog 2 spectrofluorimeter (Jobin Yvon, Lonjumeau, France) on conjugate solution in 10 mM NaCl, 50 mM Tris-HCl (pH 7.4) or 0.2 N HClO$_4$ in the presence or absence of CT-DNA.

b. Fluorescence Binding Studies. Quenching Q values were determined for CT-DNA, [poly(dA-dT)]$_2$, and [poly(dG-dC)]$_2$ (Amersham Pharmacia Biotech, Saclay, France) for solutions of 20 μM DNAp in acetate buffer (9.3 mM NaCl, 2 mM NaOAc, 0.1 mM ethylenediaminetetraacetic acid (EDTA), pH 5.0) containing 2 μM ethidium bromide as described previously.[60] The CC$_{50}$ values for ethidium displacement were determined using solutions containing 1 μM CT-DNA and 1.26 μM ethidium bromide.[58] Fluorescence (excitation at 546 nm; emission at 595 nm) was monitored in 10 mm path length quartz cuvettes using a Fluorolog 2 spectrofluorimeter following serial addition of aliquots of a stock conjugate solution. The Q and CC$_{50}$ values are defined as the conjugate concentrations reducing the fluorescence of initially DNA-bound ethidium by 50%. None of the compounds showed fluorescence at 595 nm or interfered with the fluorescence of unbound ethidium. Molar extinction values of $\epsilon_{260} = 6600, 6700$, and 8400 (M phosphate)$^{-1}$ cm^{-1}, respectively, were used for [poly(dA-dT)]$_2$, CT-DNA, and [poly(dG-dC)]$_2$.[30,75]

c. Cell Culture. Murine leukemia L1210, CHO, and CHO-MG cells were grown in RPMI 1640 medium (Eurobio, Les Ulis, France) supplemented with 10% fetal calf serum, 2 mM glutamine, penicillin (100 U/mL), and streptomycin (50 μg/mL) (BioMerieux, Marcy l'Etoile, France). l-Proline (2 μg/mL) was added to the culture medium for CHO-MG cells. Cells were grown at 37 °C under a humidified 5% CO$_2$ atmosphere. As all of the conjugates were substrates of the bovine serum amine oxidase (data not shown), 2 mM aminoguanidine was added to the culture medium to prevent any oxidative degradation of the conjugates by the enzyme present in the calf serum.

d. SPD Uptake Inhibition in L1210 and CHO Cells. The acridine derivatives were studied for their ability to compete with [^{14}C]SPD (Amersham Pharmacia Biotech) for uptake into L1210 cells in vitro. Cell suspensions (1.5 × 10^6 cells) were incubated in 0.6 mL of Hanks' balanced salt solution (HBSS) supplemented with 20 mM Hepes containing 1, 2, and 4 μM [^{14}C]SPD alone or with the additional presence of 0.025, 0.050, and 0.125 μM acridine derivative for 5 min at 37 °C. At the end of the incubation period, the cell suspensions were layered on top of a mixture of corn oil and dibutylphthalate and centrifuged.[62] Cell pellets were dissolved in 500 μL of 0.1 N NaOH. Aliquots were transferred to vials for scintillation counting. Other aliquots were used for protein determination. Lineweaver−Burke plots indicated a simple competitive inhibition with respect to SPD.

CHO cells were grown in 12 well plates. After three washings in prewarmed phosphate-buffered saline (PBS), 1 mL of a prewarmed solution of HBSS−Hepes buffer containing 1 μM [^{14}C]SPD was added to each well. When required, the solution contained various concentrations of the conjugates. After it was incubated at 37 °C for 5 min, the cells were washed three times with ice-cold PBS and lysed in 0.1 N NaOH. In some experiments, CHO cells were pretreated with 5 mM DFMO during 24 h and/or incubated for 2 h at 37 °C with various concentrations of conjugates (0.001−10 μM) in the culture medium before the uptake measurements.

e. In Vitro Evaluation of Conjugate Cytotoxicity/Cytostasy. The effects of the acridine derivatives on cell growth were assayed in sterile 96 well microtiter plates (Becton Dickinson, Oxnard, CA). L1210 cells were seeded at 5×10^4 cells/mL of medium (100 μL per well). Single CHO and CHO-MG cells, harvested by trypsinization, were plated at 2×10^3 cells/mL. Conjugate solutions (5 μL per well) of appropriate concentration were added at the time of seeding for L1210 cells and after an overnight incubation for CHO and CHO-MG cells. In some experiments, 5 mM DFMO was added to the culture medium at the time of conjugate addition. After exposure to the conjugate for 48 h, cell growth was determined by measuring formazan formation from 3-(4,5-dimethylthiazol-2-yl)2,5-diphenyltetrazolium using a Titertek Multiskan MCC/340 microplate reader (Labsystems, Cergy-Pontoise, France) for absorbance (540 nm) measurements.[76]

f. Cellular Uptake. For determination of the cellular uptake of the derivatives, cells were seeded in culture flasks at 2×10^5 cells/mL for L1210 cells and at 1×10^5 cells/mL for CHO and CHO-MG cells. Conjugates were added at the time of seeding for L1210 and 24 h after seeding for CHO and CHO-MG cells. In some experiments, 500 μM SPD was added at the time of conjugate addition.

For cellular uptake in DFMO-pretreated L1210 cells, cells were seeded at 10^5 cells/mL in culture medium containing 5 mM DFMO and conjugates were added 24 h later. For cellular uptake in DFMO-pretreated CHO and CHO-MG cells, cells were seeded at 5×10^4 cells/mL. DFMO (5 mM) was added 24 h later. After they were incubated for 48 h, conjugates were added as dilute solutions in 0.14 M NaCl.

All cells were harvested 24 h after conjugate addition. Harvested cells were washed three times in 0.14 M NaCl. Cell pellets were disrupted by sonication in 1 mL of 0.2 N HClO$_4$/2 M NaCl. After 16 h at 4 °C, homogenates were centrifuged at 15 000 rpm for 30 min. Pellets were dissolved in 0.1 N NaOH and used for protein determination with the Folin phenol reagent.[77] Conjugate concentrations in the supernatants were evaluated by fluorescence measurements using dilutions of the compounds in extraction buffer as standards. Fluorescence spectra were recorded on a Fluorolog 2 spectrofluorimeter: aminoacridine (exc: 360 nm; em: 380−500 nm); amidoacridine (exc: 410 nm; em: 420−500 nm).

References

(1) Cohen, S. S. *A Guide to the Polyamines*; Oxford University Press: New York, 1998.

(2) Pegg, A. E. Polyamine metabolism and its importance in neoplastic growth and as a target for chemotherapy. *Cancer Res.* **1988**, *48*, 759−774.

(3) Seiler, N.; Dezeure, F. Polyamines transport in mammalian cells. *Int. J. Biochem.* **1990**, *22*, 211−218.

(4) Seiler, N.; Delcros, J. G.; Moulinoux, J. P. Polyamine transport in mammalian cells. An update. *Int. J. Biochem. Cell Biol.* **1996**, *28*, 843−861.

(5) Bachrach, U.; Seiler, N. Formation of acetylpolyamines and putrescine from spermidine by normal and transformed chick embryo fibroblasts. *Cancer Res.* **1981**, *41*, 1205−1208.

(6) Chen, K. Y.; Rinehart, C. A., Jr. Difference in putrescine transport in undifferentiated versus differentiated mouse NB-15 neuroblastoma cells. *Biochem. Biophys. Res. Commun.* **1981**, *101*, 243−249.

(7) Alhonen-Hongisto, L.; Seppanen, P.; Janne, J. Intracellular putrescine and spermidine deprivation induces increased uptake of the natural polyamines and methylglyoxal bis(guanylhydrazone). *Biochem. J.* **1980**, *192*, 941−945.

(8) Minchin, R. F.; Raso, A.; Martin, R. L.; Ilett, K. F. Evidence for the existence of distinct transporters for the polyamines putrescine and spermidine in B16 melanoma cells. *Eur. J. Biochem.* **1991**, *200*, 457−462.

(9) Rinehart, C. A. J.; Chen, K. Y. Characterization of the polyamine transport system in mouse neuroblastoma cells. Effects of sodium and system A amino acids. *J. Biol. Chem.* **1984**, *259*, 4750−4756.

(10) Volkow, N.; Goldman, S. S.; Flamm, E. S.; Cravioto, H.; Wolf, A. P.; Brodie, J. D. Labeled putrescine as a probe in brain tumors. *Science* **1983**, *221*, 673−675.

(11) Heston, W. D. W.; Kadmon, D.; Covey, D. F.; Fair, W. R. Differential effect of α-difluoromethylornithine on the in vivo uptake of ^{14}C-labeled polyamines and methylglyoxal bis-(guanylhydrazone) by a rat prostate-derived tumor. *Cancer Res.* **1984**, *44*, 1034−1040.

(12) Chaney, J. E.; Kobayashi, K.; Goto, R.; Digenis, G. A. Tumor selective enhancement of radioactivity uptake in mice treated with alpha-difluoromethylornithine prior to administration of 14C-putrescine. *Life Sci.* **1983**, *32*, 1237−1241.

(13) Redgate, E. S.; Grudziak, A. G.; Deutsch, M.; Boggs, S. S. Difluoromethylornithine enhanced uptake of tritiated putrescine in 9L rat brain tumors. *Int. J. Radiat. Oncol. Biol. Phys.* **1997**, *38*, 169−174.

(14) Holley, J. L.; Mather, A.; Wheelhouse, R. T.; Cullis, P. M.; Hartley, J. A.; Bingham, J. P.; Cohen, G. M. Targeting of tumor cells and DNA by a chlorambucil-spermidine conjugate. *Cancer Res.* **1992**, *52*, 4190−4195.

(15) Cullis, P. M.; Merson-Davies, L.; Weaver, R. Mechanism and reactivity of chlorambucil and chlorambucil-spermidine conjugate. *J. Am. Chem. Soc.* **1995**, *117*, 8033−8034.

(16) Stark, P. A.; Thrall, B. D.; Meadows, G. G.; Abdel-Monem, M. M. Synthesis and evaluation of novel spermidine derivatives as targeted cancer chemotherapeutic agents. *J. Med. Chem.* **1992**, *35*, 4264−4269.

(17) Holley, J.; Mather, A.; Cullis, P.; Symons, M. R.; Wardman, P.; Watt, R. A.; Cohen, G. M. Uptake and cytotoxicity of novel nitroimidazole-polyamine conjugates in Ehrlich ascites tumour cells. *Biochem. Pharmacol.* **1992**, *43*, 763−769.

(18) Heston, W. D.; Uy, L.; Fair, W. R.; Covey, D. F. Cytotoxic activity of aziridinyl putrescine enhanced by polyamine depletion with alpha-difluoromethylornithine. *Biochem. Pharmacol.* **1985**, *34*, 2409−2410.

(19) Yuan, Z. M.; Egorin, M. J.; Rosen, D. M.; Simon, M. A.; Callery, P. S. Cellular pharmacology of N1- and N8-aziridinyl analogues of spermidine. *Cancer Res.* **1994**, *54*, 742−748.

(20) Eiseman, J. L.; Rogers, F. A.; Guo, Y.; Kauffman, J.; Sentz, D. L.; Klinger, M. F.; Callery, P. S.; Kyprianou, N. Tumor-targeted apoptosis by a novel spermine analogue, 1,12-diaziridinyl-4,9-diazadodecane, results in therapeutic efficacy and enhanced radiosensitivity of human prostate cancer. *Cancer Res.* **1998**, *58*, 4864−4870.

(21) Huber, M.; Pelletier, J. G.; Torossian, K.; Dionne, P.; Gamache, I.; Charestgandreault, R.; Audette, M.; Poulin, R. 2,2′-Dithiobis(N-ethyl-spermine-5-carboxamide) is a high affinity, membrane-impermeant antagonist of the mammalian polyamine transport system. *J. Biol. Chem.* **1996**, *271*, 27556−27563.

(22) Byers, T. L.; Pegg, A. E. Regulation of polyamine transport in Chinese hamster ovary cells. *J. Cell. Physiol.* **1990**, *143*, 460−467.

(23) Muller, S.; Luchow, A.; McCann, P. P.; Walter, R. D. Effect of bis(benzyl)polyamine derivatives on polyamine transport and survival of Brugia pahangi. *Parasitol. Res.* **1991**, *77*, 612−615.

(24) Marton, L. J.; Levin, V. A.; Hervatin, S. J.; Koch-Weser, J.; McCann, P. P.; Sjoerdsma, A. Potentiation of the antitumor therapeutic effects of 1,3-bis(2-chloroethyl)-1-nitrosourea by alpha-difluoromethylornithine, an ornithine decarboxylase inhibitor. *Cancer Res.* **1981**, *41*, 4426−4431.

(25) Aziz, S. M.; Yatin, M.; Worthen, D. R.; Lipke, D. W.; Crooks, P. A. A novel technique for visualizing the intracellular localization and distribution of transported polyamines in cultured pulmonary artery smooth muscle cells. *J. Pharm. Biomed. Anal.* **1998**, *17*, 307−320.

(26) Demeunynck, M.; Charmantray, F.; Martelli, A. Interest of acridine derivatives in the anticancer chemotherapy. *Curr. Pharm. Des.* **2001**, *7*, 1703−1724.

(27) Edwards, M. L.; Snyder, R. D.; Stemerick, D. M. Synthesis and DNA-binding properties of polyamine analogues. *J. Med. Chem.* **1991**, *34*, 2414−2420.

(28) Feuerstein, B. G.; Williams, L. D.; Basu, H. S.; Marton, L. J. Implications and concepts of polyamine-nucleic acid interactions. *J. Cell. Biochem.* **1991**, *46*, 37−47.

(29) Cohen, G. N.; Cullis, P. M.; Hartley, J. A.; Mather, A.; Symons, M. C. R.; Wheelhouse, R. T. Targeting of cytotoxic agents by polyamines-synthesis of a chlorambucil spermidine conjugate. *J. Chem. Soc. Chem. Commun.* **1992**, 298−300.

(30) Rodger, A.; Blagbrough, I. S.; Adlam, G.; Carpenter, M. L. DNA binding of a spermine derivative: Spectroscopic study of anthracene-9-carbonyl-N-1-spermine with poly[d(G−C).d(G−C)] and poly[d(A−T).d(A−T)]. *Biopolymers* **1994**, *34*, 1583−1593.

(31) Rodger, A.; Taylor, S.; Adlam, G.; Blagbrough, I. S.; Haworth, I. S. Multiple DNA binding modes of anthracene-9-carbonyl-N1-spermine. *Bioorg. Med. Chem.* **1995**, *3*, 861−872.

(32) Blagbrough, I. S.; Taylor, S.; Carpenter, M. L.; Novoselskiy, V.; Shamma, T.; Haworth, I. S. Asymmetric intercalation of *N*¹-(acridin-9-ylcarbonyl)spermine at homopurine sites of duplex DNA. *Chem. Commun.* **1998**, 929−930.

(33) Phanstiel, O. I.; Price, H. L.; Wang, L.; Juusola, J.; Kline, M.; Shah, S. M. The effect of polyamine homologation on the transport and cytotoxicity properties of polyamine-(DNA-intercalator) conjugates. *J. Org. Chem.* **2000**, *65*, 5590−5599.

(34) Wang, L.; Price, H. L.; Juusola, J.; Kline, M.; Phanstiel, O. I. Influence of polyamine architecture on the transport and topoisomerase II inhibitory properties of polyamine DNA-intercalator conjugates. *J. Med. Chem.* **2001**, *44*, 3682−3691.

(35) Bergeron, R. J.; Feng, Y.; Weimar, W. R.; McManis, J. S.; Dimova, H.; Porter, C.; Raisler, B.; Phanstiel, O. A comparison of structure−activity relationships between spermidine and spermine analogue antineoplastics. *J. Med. Chem.* **1997**, *40*, 1475−1494.

(36) Siddiqui, A. Q.; Merson-Davies, L.; Cullis, P. M. The synthesis of novel polyamine-nitroimidazole conjugates designed to probe the structural specificities of the polyamine uptake system in A549 lung carcinoma cells. *J. Chem. Soc. Trans.* **1999**, *1*, 3243−3252.

(37) Cullis, P. M.; Green, R. E.; Merson-Davies, L.; Travis, N. Probing the mechanism of transport and compartmentalisation of polyamines in mammalian cells. *Chem. Biol.* **1999**, *6*, 717−729.

(38) Martin, B.; Possémé, F.; Le Barbier, C.; Carreaux, F.; Carboni, B.; Seiler, N.; Moulinoux, J. P.; Delcros, J. G. N-benzylpolyamines as vectors of boron and fluorine for cancer therapy and imaging: Synthesis and biological evaluation. *J. Med. Chem.* **2001**, *44*, 3653−3664.

(39) Porter, C. W.; Miller, J.; Bergeron, R. J. Aliphatic chain length specificity of the polyamine transport system in ascites L1210 leukemia cells. *Cancer Res.* **1984**, *44*, 126−128.

(40) Bergeron, R. J.; McManis, J. S.; Weimar, W. R.; Schreier, K. M.; Gao, F.; Wu, Q.; Ortiz-Ocasio, J.; Luchetta, G. R.; Porter, C.; Vinson, J. R. The role of charge in polyamine analogue recognition. *J. Med. Chem.* **1995**, *38*, 2278−2285.

(41) Mancuso, A. J.; Huang, S. L.; Swern, D. Oxidation of long-chain and related alcohols to carbonyl by dimethyl sulfoxide "activated" by oxalyl chloride. *J. Org. Chem.* **1978**, *43*, 2480−2482.

(42) Moya, E.; Blagbrough, I. S. Total syntheses of polyamine amides PhTX-4.3.3 and PhTX-3.4.3: Reductive alkylation is a rapid, practical route to philanthotoxins. *Tetrahedron Lett.* **1995**, *36*, 9401−9404.

(43) Ashton, M. R.; Moya, E.; Blagbrough, I. S. Total synthesis of modified JSTX toxins: Reductive alkylation is a practical route to hexahydropyrimidine polyamine amides. *Tetrahedron Lett.* **1995**, *36*, 9397−9400.

(44) Lucente, G.; Pinnen, F.; Zanotti, G. A new method for oxidative decarboxylation of N-acyl-α-amino acids and peptides. *Tetrahedron Lett.* **1978**, *34*, 3155−3158.

(45) Shono, T.; Matsumura, Y.; Kanasawa, T.; Habuka, M.; Unchida, K.; Toyoda, K. Electro-organic chemistry. Part 80. α-hydroxylation of *N*-acylated cyclic amine and utilization of the products as amino-aldehyde equivalents. *J. Chem. Res.* **1984**, *S*, 320−321.

(46) Nagasaka, T.; Tamano, H.; Maekawa, T.; Hamaguchi, F. Introduction of functional groups into the α-position of N-alkoxycarbonylpyrrolidines. *Heterocycles* **1987**, *26*, 617−625.

(47) Quibell, M.; Turnell, W. G.; Johnson, T. Synthesis of azapeptides by the Fmoc/*tert*-butyl/polyamide technique. *J. Chem. Soc. Perkin Trans. 1* **1993**, 2843−2849.

(48) Takeuchi, Y.; Takagi, S. I.; Tokuda, S. I.; Koike, M.; Abe, H.; Harayama, T.; Shibata, K.; Kim, H. S.; Wataya, Y. Synthesis and antimalarial activity of *DL*-deoxyfebrifugine. *Heterocycles* **1999**, *51*, 1869−1875.

(49) Blagbrough, I. S.; Geall, A. J. Practical synthesis of unsymmetrical polyamine amides. *Tetrahedron Lett.* **1998**, *39*, 439−442.

(50) Dupre, D. J.; Robinson, F. A. N-Substituted 5-aminoacridines. *J. Chem. Soc.* **1945**, 549−551.

(51) Ghaneolhosseini, H.; Tjarks, W.; Sjoberg, S. Synthesis of novel boronated acridines- and spermidines as possible agents for BNCT. *Tetrahedron* **1998**, *54*, 3877−3884.

(52) Qarawi, M. A.; Carrington, S.; Blagbrough, I. S.; Moss, S. H.; Pouton, C. W. Optimization of the MTT assay for B16 murine melanoma cells and its application in assessing growth inhibition by polyamines and novel polyamine conjugates. *Pharm. Sci.* **1997**, *3*, 235−239.

(53) Schreiber, J. P.; Daune, M. P. Fluorescence of complexes of acridine dye with synthetic polydeoxyribonucleotides: a physical model of frameshift mutation. *J. Mol. Biol.* **1974**, *83*, 487−501.

(54) Hansen, J. B.; Koch, T.; Buchardt, O.; Nielsen, P. E.; Norden, B. M. W. Trisintercalation in DNA by N-[3-(9-acridinylamino)-propyl]-N,N-bis[6-(9-acridinylamino)hexyl]amine. *J. Chem. Soc. Chem. Commun.* **1984**, 509−511.

(55) Krey, A. K.; Hahn, F. E. Studies on the complex of distamycin a with calf thymus DNA. *FEBS Lett.* **1970**, *10*, 175−178.

(56) Dougherty, G.; Pilbrow, J. R. Physicochemical probes of intercalation. *Int. J. Biochem.* **1984**, *16*, 1179−1192.

(57) Morgan, A.; Lee, J. S.; Pulleyblank, D. E.; Murray, N. L.; Evans, D. H. Review: ethidium fluorescence assays. Part 1. Physicochemical studies. *Nucleic Acids Res.* **1979**, *7*, 547−569.

(58) McConnaughie, A. W.; Jenkins, T. C. Novel acridine-triazenes as prototype combilexins: synthesis, DNA binding, and biological activity. *J. Med. Chem.* **1995**, *38*, 3488−3501.

(59) Baguley, B. C. Nonintercalative DNA-binding antitumour compounds. *Mol. Cell. Biochem.* **1982**, *43*, 167−181.

(60) Bailly, C.; Pommery, N.; Houssin, R.; Henichart, J. P. Design, synthesis, DNA binding, and biological activity of a series of DNA minor-groove-binding intercalating drugs. *J. Pharm. Sci.* **1989**, *78*, 910−917.

(61) Antonini, I.; Polucci, P.; Jenkins, T. C.; Kelland, L. R.; Menta, E.; Pescalli, N.; Stefanska, B.; Mazerski, J.; Martelli, S. 1-[(ω-aminoalkyl)amino]-4-[N-(ω-aminoalkyl)carbamoyl]-9-oxo-9,10-dihydroacridines as intercalating cytotoxic agents: synthesis, DNA binding, and biological evaluation. *J. Med. Chem.* **1997**, *40*, 3749−3755.

(62) Seiler, N.; Douaud, F.; Renault, J.; Delcros, J. G.; Havouis, R.; Uriac, P.; Moulinoux, J. P. Polyamine sulfonamides with NMDA antagonist properties are potent calmodulin antagonists and cytotoxic agents. *Int. J. Biochem. Cell Biol.* **1998**, *30*, 393−406.

(63) Tomasi, S.; Le Roch, M.; Renault, J.; Corbel, J. C.; Uriac, P.; Carboni, B.; Moncoq, D.; Martin, B.; Delcros, J. G. Solid-phase organic synthesis of polyamine derivatives and initial biological evaluation of their antitumoral activity. *Bioorg. Med. Chem. Lett.* **1998**, *8*, 635−640.

(64) Delcros, J. G.; Vaultier, M.; LeRoch, N.; Havouis, R.; Moulinoux, J. P.; Seiler, N. Bis(7-amino-4-azaheptyl)dimethylsilane: A new tetramine with polyamine-like features. Effects on cell growth. *Anticancer Drug Des.* **1997**, *12*, 35−48.

(65) Porter, C. W.; Ganis, B.; Vinson, T.; Marton, L. J.; Kramer, D. L.; Bergeron, R. J. Comparison and characterization of growth inhibition in L1210 cells by alpha-difluoromethylornithine, an inhibitor of ornithine decarboxylase, and N1,N8-bis(ethyl)-spermidine, an apparent regulator of the enzyme. *Cancer Res.* **1986**, *46*, 6279−6285.

(66) Byers, T. L.; Pegg, A. E. Properties and physiological function of the polyamine transport system. *Am. J. Physiol.* **1989**, *257*, C545−C553.

(67) Mitchell, J. L.; Diveley, R. R., Jr.; Bareyal-Leyser, A. Feedback repression of polyamine uptake into mammalian cells requires active protein synthesis. *Biochem. Biophys. Res. Commun.* **1992**, *186*, 81−88.

(68) Kramer, D. L.; Miller, J. T.; Bergeron, R. J.; Khomutov, R.; Khomutov, A.; Porter, C. W. Regulation of polyamine transport by polyamines and polyamine analogues. *J. Cell. Physiol.* **1993**, *155*, 399−407.

(69) Mi, Z.; Kramer, D. L.; Miller, J. T.; Bergeron, R. J.; Bernacki, R.; Porter, C. W. Human prostatic carcinoma cell lines display altered regulation of polyamine transport in response to polyamine analogues and inhibitors. *Prostate* **1998**, *34*, 51−60.

(70) Weeks, R. S.; Vanderwerf, S. M.; Carlson, C. L.; Burns, M. R.; O'Day, C. L.; Cai, F.; Devens, B. H.; Webb, H. K. Novel lysine-spermine conjugate inhibits polyamine transport and inhibits cell growth when given with DFMO. *Exp. Cell Res.* **2000**, *261*, 293−302.

(71) Heston, W. D.; Charles, M. Calmodulin antagonist inhibition of polyamine transport in prostatic cancer cells in vitro. *Biochem. Pharmacol.* **1988**, *37*, 2511−2514.

(72) Khan, N. A.; Sezan, A.; Quemener, V.; Moulinoux, J. P. Polyamine transport regulation by calcium and calmodulin: role of Ca(2+)-ATPase. *J. Cell. Physiol.* **1993**, *157*, 493−501.

(73) Scemama, J. L.; Grabie, V.; Seidel, E. R. Characterization of univectorial polyamine transport in duodenal crypt cell line. *Am. J. Physiol.* **1993**, *265*, G851−G856.

(74) Louwrier, S.; Tuynman, A.; Hiemstra, H. Synthesis of bicyclic guanidines from pyrrolidin-2-one. *Tetrahedron* **1996**, *52*, 2629−2646.

(75) Delcros, J. G.; Sturkenboom, M. C.; Basu, H. S.; Shafer, R. H.; Szollosi, J.; Feuerstein, B. G.; Marton, L. J. Differential effects of spermine and its analogues on the structures of polynucleotides complexed with ethidium bromide. *Biochem. J.* **1993**, *291*, 269−274.

(76) Mosmann, T. Rapid colorimetric assay for cellular growth and survival: application to proliferation and cytotoxicity assays. *J. Immunol. Methods* **1983**, *65*, 55−63.

(77) Lowry, O. H.; Rosenbrough, N. J.; Farr, A. L.; Randall, R. J. Protein measurement with the Folin phenol reagent. *J. Biol. Chem.* **1951**, *193*, 265−275.